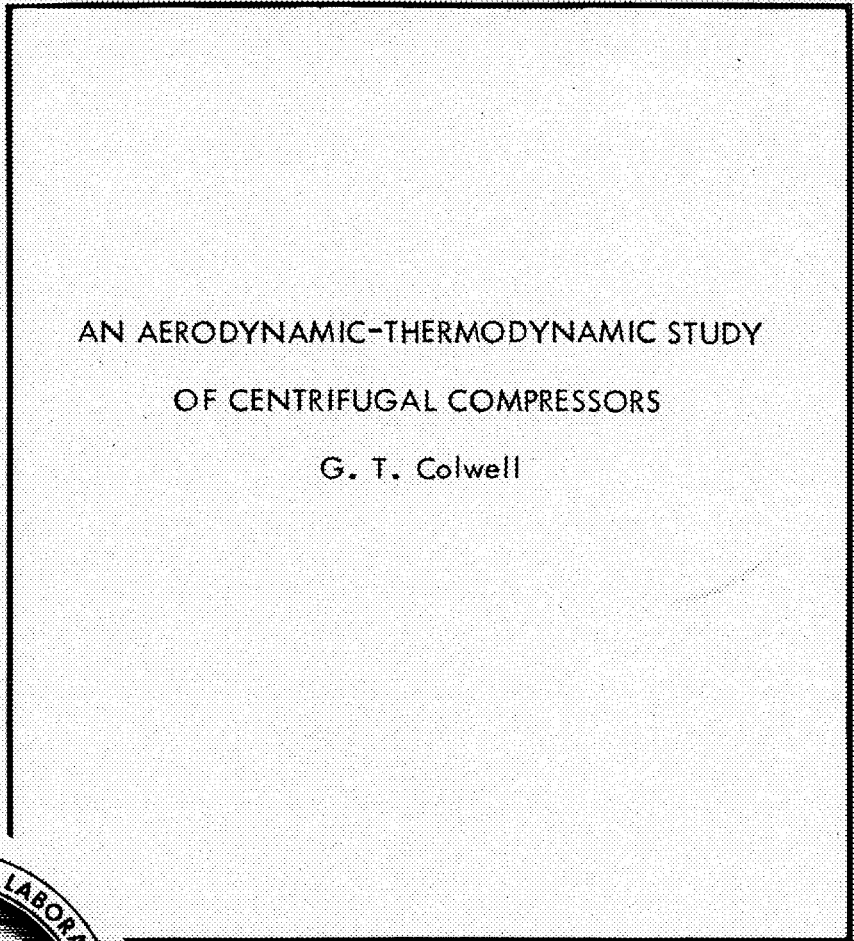


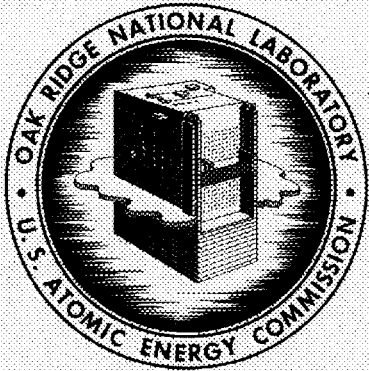
128

ORNL  
MASTER COPY

ORNL-3294 *Def*  
UC-80 - Reactor Technology



AN AERODYNAMIC-THERMODYNAMIC STUDY  
OF CENTRIFUGAL COMPRESSORS  
G. T. Colwell



**OAK RIDGE NATIONAL LABORATORY**  
operated by  
**UNION CARBIDE CORPORATION**  
for the  
**U. S. ATOMIC ENERGY COMMISSION**

Printed in USA. Price: \$2.00 Available from the  
Office of Technical Services  
U. S. Department of Commerce  
Washington 25, D. C.

#### LEGAL NOTICE

This report was prepared as an account of Government sponsored work. Neither the United States, nor the Commission, nor any person acting on behalf of the Commission:

- A. Makes any warranty or representation, expressed or implied, with respect to the accuracy, completeness, or usefulness of the information contained in this report, or that the use of any information, apparatus, method, or process disclosed in this report may not infringe privately owned rights; or
- B. Assumes any liabilities with respect to the use of, or for damages resulting from the use of any information, apparatus, method, or process disclosed in this report.

As used in the above, "person acting on behalf of the Commission" includes any employee or contractor of the Commission, or employee of such contractor, to the extent that such employee or contractor of the Commission, or employee of such contractor prepares, disseminates, or provides access to, any information pursuant to his employment or contract with the Commission, or his employment with such contractor.

ORNL-3294

UC-80 -- Reactor Technology  
TID-4500 (18th ed.)

Contract No. W-7405-eng-26

Reactor Division

AN AERODYNAMIC-THERMODYNAMIC STUDY  
OF CENTRIFUGAL COMPRESSORS

G. T. Colwell

DATE ISSUED

DEC 4 1962

OAK RIDGE NATIONAL LABORATORY  
Oak Ridge, Tennessee  
operated by  
UNION CARBIDE CORPORATION  
for the  
U. S. ATOMIC ENERGY COMMISSION



## CONTENTS

	<u>Page</u>
ABSTRACT .....	v
NOMENCLATURE .....	vii
1. INTRODUCTION .....	1
2. IMPELLER DESIGN .....	2
Impeller Analysis .....	2
Head Corresponding to Pressure Rise .....	2
Inlet Specific Speed .....	4
Isentropic Work Rate Required .....	5
Inlet Velocity Triangle .....	5
Speed of Vanes at Inlet .....	6
Value for Exit Blade Angle, $\beta^2$ .....	8
Outside Diameter of the Impeller .....	8
Number of Blades Needed .....	14
Slip Between Fluid and Impeller at Outlet .....	15
Outlet Velocity Triangle .....	15
Check of Outer Diameter Calculation .....	17
Impeller Outlet Static Pressure Head and Outlet Static Pressure .....	21
Impeller Exit Temperature .....	22
Vane Height at Inlet and Outlet .....	23
Velocity Distribution Along Driving Face of Vanes ....	25
Impeller Layout .....	30
3. CASING DESIGN .....	33
Volute Design .....	33
Volute Tongue Diameter.....	33
Average Casing Velocity .....	34
Volute Outlet Area and Diffuser Inlet Area .....	36
Static Pressure and Temperature in the Volute .....	36
Diffuser Design .....	38
Diffuser Angle .....	38
Inlet and Outlet Areas for Diffuser .....	38
Length of the Diffuser ( $L_D$ ) .....	40

4. PREDICTION OF HEAD-FLOW CURVES .....	41
Outline of Method .....	41
Friction Losses .....	42
Loss of Conversion from Velocity to Pressure .....	43
Additional Loss in the Volute .....	44
Entrance Loss .....	44
Output Head Coefficient .....	44
5. SURGING IN CENTRIFUGAL COMPRESSORS .....	47
6. EXAMPLE OF AN IMPELLER DESIGN .....	48
7. EXAMPLE OF A CASING DESIGN .....	64
Volute Design .....	64
Diffuser Design .....	67
8. SUMMARY .....	73
ACKNOWLEDGMENTS .....	74
BIBLIOGRAPHY .....	75

## ABSTRACT

A procedure is presented for the aerodynamic and thermodynamic design of centrifugal compressors. Design equations are derived from basic laws of thermodynamics and fluid flow where possible. The experimental data and much of the mathematical treatment comes from the extensive literature on centrifugal compressors. An attempt has been made to assemble the bits of information which were available into a logical design method. The available information has been supplemented with mathematical developments and explanations which seemed necessary to complete the general view of centrifugal compressor design. Of particular interest is the derivation, using the work of Stanitz and Ellis (NACA Report 954) as a starting point, of equations which provide for estimating the velocity distribution on the leading edge of an impeller vane. Also included is an example of an aerodynamic-thermodynamic design of an impeller and a volute-conical diffuser combination. All the necessary steps are demonstrated, beginning with a set of basic compressor requirements and resulting in a layout of the impeller and casing.



## NOMENCLATURE

A	Area
C	Heat capacity, velocity of sound
$C_p$	Specific heat
D	Diameter
E	Energy
F	Force
H,h	Head, enthalpy, vane height
J	Conversion factor
K,k	Flow coefficient, specific heat ratio
L	Length
M,m	Mach number, mass flow rate
N	Rotational speed
$N_s$	Specific speed
P,p	Power, pressure
Q,q	Volume flow rate, heat transfer, relative velocity
R	Gas constant
S	Slip factor
T,t	Absolute temperature, blade thickness
U,u	Internal energy, tangential component of relative velocity
V,v	Velocity, specific volume, radial component of relative velocity
W,w	Work
X	Flow ratio
Z,z	Compressibility factor, number of blades
$\alpha$	Cone angle
$\beta$	Blade angle
$\gamma$	Blade angle
$\Delta$	Finite change in; angle
$\delta$	Diameter ratio
$\epsilon$	Radius ratio
$\eta$	Efficiency
$\theta$	Angle on fluid element; volute angle
$\lambda$	Leakage factor

$\xi$	Angle factor
$\rho$	Density
$\sigma$	Velocity distribution factor
$\tau$	Torque
$\phi$	Flow coefficient
$\psi$	Head coefficient
$\omega$	Angular velocity

### Subscripts

1	Vane inlet
2	Vane exit
L	Local
c	Constant; critical
R	Ratio
o	Inlet pipe; stagnation state
I	Ideal
U	Tangential
S	Isentropic
d	Driving face
a	Average
N	Per blade
r	Radial
v	Volute
D	Diffuser
f	Friction
i	Input
$\infty$	Average
$\theta$	Tangential
e	Entrance
x	Flow ratio

## 1. INTRODUCTION

A procedure has been developed for aerodynamic-thermodynamic design of centrifugal compressors based on recent advances in fluid flow and aerodynamic technology. Only those parts of a compressor that guide or add energy to the working fluid are discussed. Only a short discussion of transient operations is presented to introduce problems of surge and system response of which the designer should be aware.

The procedures outlined are intended to be sufficiently general to hold for most gases at a wide range of specific speeds. The equations presented are applicable to compressible fluids in the sense that they deviate from an ideal gas and that they can support little shear. No account is taken in the analysis of Mach number effects, since most compressors operate in flow regimes where Mach number effects are unimportant (inlet Mach number less than 0.8). With some modifications, however, the methods discussed could be used for the design of centrifugal pumps.

Step by step procedures are given for the design of an impeller and volute. Also included is a design that is intended to illustrate the use of the methods presented. An effort has been made to utilize the research of a great many investigators to provide a sound basis for the ideas presented.

## 2. IMPELLER DESIGN

Normally when an impeller for a centrifugal compressor is to be designed, some or all of the following conditions are known: (1) type of gas, (2) inlet temperature and pressure, (3) flow rate (either mass or volume rate), (4) pressure rise or head, and (5) impeller rotational speed. The problem then is to design a wheel that will produce the required pressure rise and flow rate at the given speed and with the specified conditions at the inlet. A mathematical analysis must first be made to determine the various dimensions of the impeller. With these dimensions a layout is made, and the necessary modifications are made to facilitate machining and assembly of the complete compressor. The steps in the design procedure are discussed below in the order in which they should be done.

### Impeller Analysis

#### Head Corresponding to Pressure Rise

The equation for the head corresponding to the pressure rise must be selected and applied carefully, particularly when the ratio of the vane exit pressure to the vane inlet pressure ( $p_2/p_1$ ) is small, i.e., slightly greater than one. The equation used here is derived from the first law of thermodynamics.

For steady flow per unit of mass flowing, the first law can be written as follows:

$$\Delta q = \Delta h + \Delta kE + \Delta z + \Delta w \quad . \quad (1)$$

The gas is in the compressor only a very short time, and therefore the compression can be considered adiabatic. If it is assumed also that the process is reversible and that there are no changes in potential energy and no changes in kinetic energy,

$$-\Delta w = h_2 - h_1 \quad . \quad (2)$$

Assuming the gas to be ideal permits Eq. (3) to be written as a total differential, since enthalpy is a function only of temperature for an ideal gas:

$$dh = C_p dT \quad . \quad (3)$$

Assuming that  $C_p$  is a constant, or using a mean value,

$$h_2 - h_1 = C_p(T_2 - T_1) \quad . \quad (4)$$

With these assumptions, the gas must obey the ideal gas equation of state and also the isentropic process equations:

$$v = \frac{RT}{P} \quad . \quad (5)$$

and

$$pv^k = p_1v_1^k = \text{constant}. \quad (6)$$

Then

$$p_1 \left( \frac{RT_1}{p_1} \right)^k = p_2 \left( \frac{RT_2}{p_2} \right)^k \quad , \quad (7)$$

$$\frac{T_2}{T_1} = \left( \frac{p_1}{p_2} \right)^{(1-k)/k} \quad , \quad (8)$$

$$-\Delta w = JT_1 C_p \left( \frac{T_2}{T_1} - 1 \right) \quad , \quad (9)$$

and

$$-\Delta w = J C_p \left[ \left( \frac{p_1}{p_2} \right)^{(1-k)/k} - 1 \right] . \quad (10)$$

But

$$H = - \frac{g_c}{g_L} \Delta w , \quad (11)$$

where H is the head rise corresponding to the pressure rise. Then

$$H = J \frac{g_c}{g_L} T_1 C_p \left[ \left( \frac{p_1}{p_2} \right)^{(1-k)/k} - 1 \right] , \quad (12)$$

where

- H = head rise, ft,
- J = conversion factor, ft·lb<sub>f</sub>/Btu,
- T<sub>1</sub> = inlet temperature, °R,
- C<sub>p</sub> = specific heat, Btu/lb<sub>m</sub>·°R,
- g<sub>c</sub> = dimensional constant, ft·lb<sub>m</sub>/lb<sub>f</sub>·sec<sup>2</sup>,
- g<sub>L</sub> = local acceleration of gravity, ft/sec<sup>2</sup>,
- p<sub>1</sub> = inlet pressure, psia,
- p<sub>2</sub> = exit pressure, psia,
- k = specific heat ratio.

The term  $g_c/g_L$  in most cases is equal to one. In aircraft, missiles, or satellites, where acceleration forces are likely to change with position or time or both,  $g_L$  is also likely to change. Since  $g_c$  is a dimensional constant, it never changes. For this reason, the ratio is included in the general equation.

#### Inlet Specific Speed

Specific speed is a similarity parameter that can be derived with the aid of dimensional analysis (21).<sup>\*</sup> It is one of the first parameters which

---

<sup>\*</sup>Numbers in parentheses refer to entries in the Bibliography.

is computed, since it gives a good indication of efficiency and compressor geometry:

$$N_s = \frac{NQ^{1/2}}{H^{3/4}}, \quad (13)$$

where

$N$  = rotational speed, rpm,

$Q$  = flow rate, fpm,

$H$  = head, ft.

#### Isentropic Work Rate Required

The isentropic work rate required is given by the expression

$$P = \frac{mH}{550} \frac{g_L}{g_c}, \quad (14)$$

where

$P$  = work rate, hp,

$m$  = mass flow rate,  $\text{lb}_m/\text{sec}$ ,

$H$  = head, ft.

#### Inlet Velocity Triangle

The inlet pipe diameter may or may not be known. If it is not known, it must be chosen. In general, an inlet velocity of between 75 and 200 fps is considered good practice (10). Velocities in this range normally give a reasonable inlet velocity triangle. The inlet velocity should be chosen so that the height of the impeller passages are not too small or too great and the inlet Mach numbers are not too large ( $<0.8$ ).

The inlet pipe velocity is given by

$$V_o = \frac{m}{\rho_1 A_o}, \quad (15)$$

where

$$\rho_1 = \frac{p_1}{ZRT_1} = \text{inlet density, lb}_m/\text{ft}^3,$$

$$p_1 = \text{inlet pressure, psia,}$$

$$T_1 = \text{inlet temperature, } ^\circ\text{R,}$$

$$R = \text{gas constant, ft}\cdot\text{lb}_f/\text{lb}_m\cdot^\circ\text{R,}$$

$$Z = \text{compressibility factor (see Fig. 1).}$$

The impeller inlet velocity is given by

$$V = \lambda V_o \quad , \quad (16)$$

where

$$V = \text{impeller inlet velocity, fps,}$$

$$\lambda = \text{leakage factor resulting from leakage from volute back to impeller inlet [conservative estimate: } \lambda = 1.03, \text{ i.e., } 3\% \text{ leakage (10)].}$$

#### Speed of Vanes at Inlet

It is desirable to make a cross-section sketch of the transition from pipe to blade inlet so that a reasonable inlet radius can be chosen. The assumed inlet radius may have to be changed when the layout is made if the passage turns too sharply, since large losses could occur. The tangential inlet tip velocity is given by

$$U_1 = r_1 \omega \quad , \quad (17)$$

where

$$r_1 = \text{vane inlet radius, ft,}$$

$$\omega = \text{angular velocity, rad/sec.}$$

The inlet relative velocity is illustrated in Fig. 2, in which

$$v_1 = [(V_1)^2 + (U_1)^2]^{1/2} \quad (18)$$

and

$$\beta_1 = \arctan \frac{V_1}{U_1} \quad , \quad (19)$$

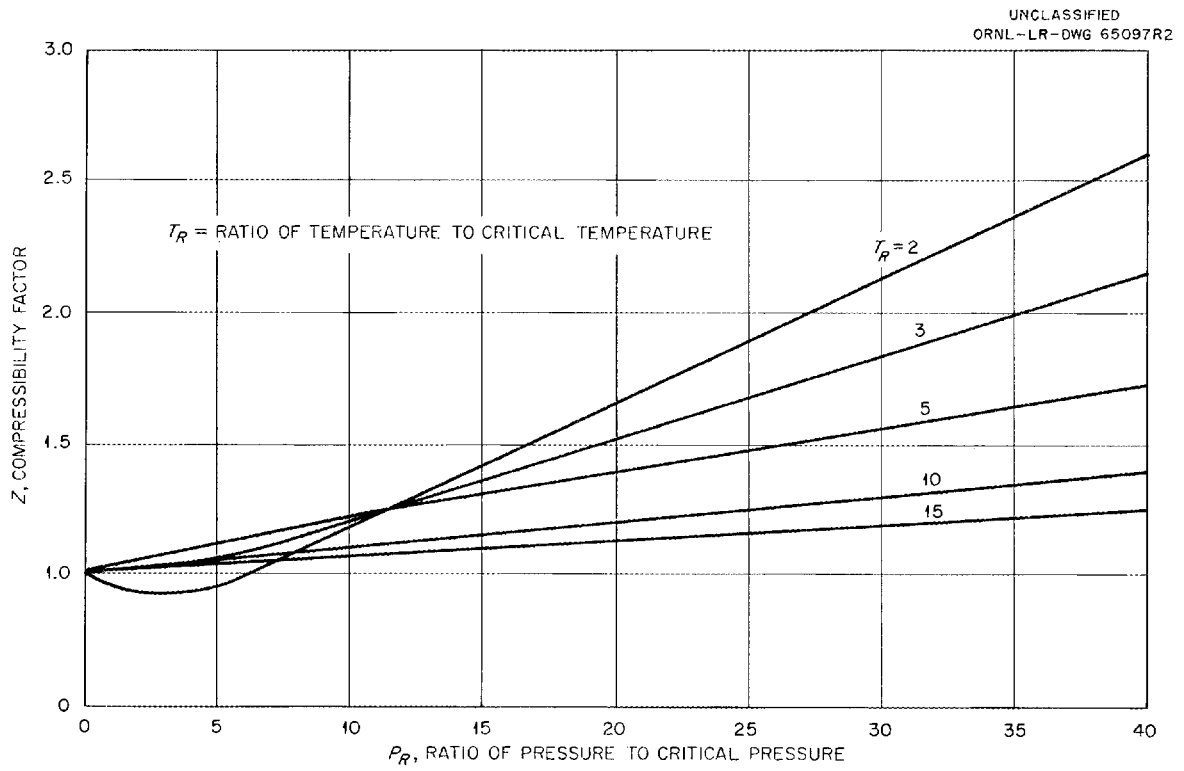


Fig. 1. Compressibility Factor Chart [Stepanoff (32)].

UNCLASSIFIED  
ORNL-LR-DWG 71571

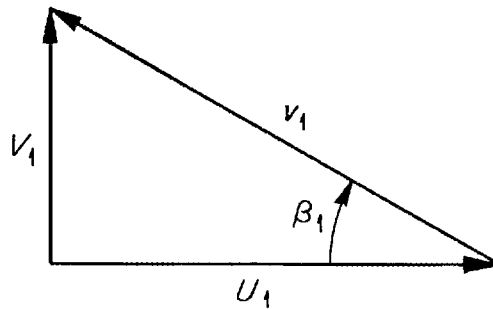


Fig. 2. Inlet Velocity Triangle.

where

$v_1$  = inlet relative velocity, fps,

$\beta_1$  = inlet blade angle, deg.

#### Value for Exit Blade Angle, $\beta_2$

The exit blade angle is probably the most important single variable in a centrifugal compressor. It determines to a large extent the head rise through the machine. This is illustrated in Fig. 3. The efficiency of a centrifugal compressor also depends strongly on the exit blade angle. This is illustrated in Fig. 4. The best efficiency is usually obtained when the exit angle is about  $60^\circ$ . However, for a given diameter the head rise will be a maximum for an exit angle of  $90^\circ$ . The change in the blower characteristic curve must also be considered for changes in exit angle. A typical head versus flow curve is shown in Fig. 5.

#### Outside Diameter of the Impeller

The approximate diameter versus head equation is used to estimate the diameter required for a given head rise. By use of the following equation, which is derived later,

$$H_I = \frac{1}{2g_L} \left( V_2'^2 - V_1^2 + U_2^2 - U_1^2 + v_1^2 - v_2'^2 \right) ,$$

and the law of cosines, with the relations shown in Fig. 6,

$$v_2'^2 = U_2^2 + V_2'^2 - 2U_2V_2' \cos \gamma_2' , \quad (20)$$

$$V_1^2 = U_1^2 + V_1^2 - 2U_1V_1 \cos \gamma_1 , \quad (21)$$

it can be seen that

$$H_I = \frac{1}{2g_L} \left( V_2'^2 - V_1^2 + U_2^2 - U_1^2 + V_1^2 - 2U_1V_1 \cos \gamma_1 - \right. \\ \left. - U_2^2 - V_2'^2 + 2U_2V_2' \cos \gamma_2' \right) , \quad (22)$$

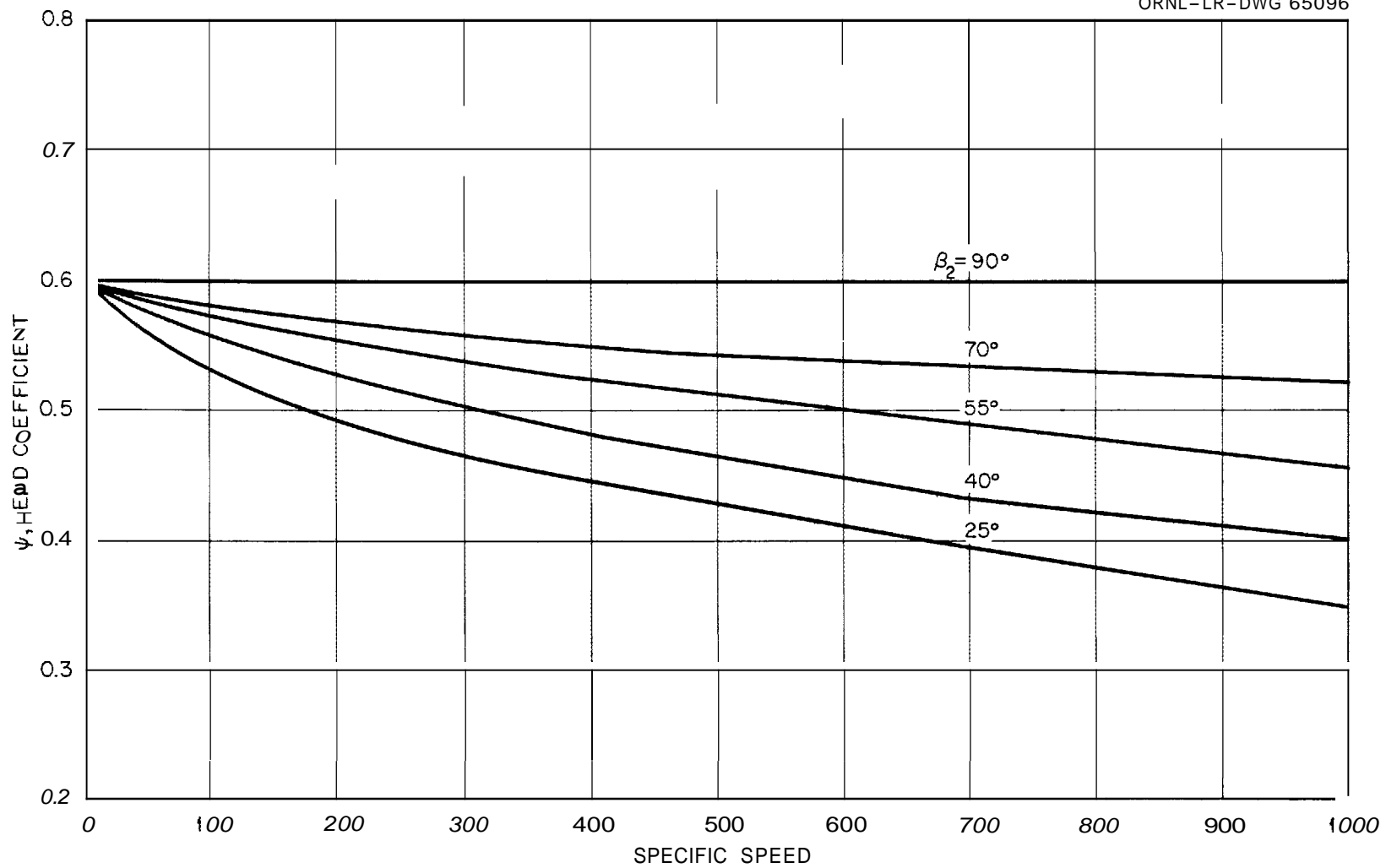


Fig. 3. Head Coefficient vs Specific Speed for Several Exit Angles [Stepanoff (32)].

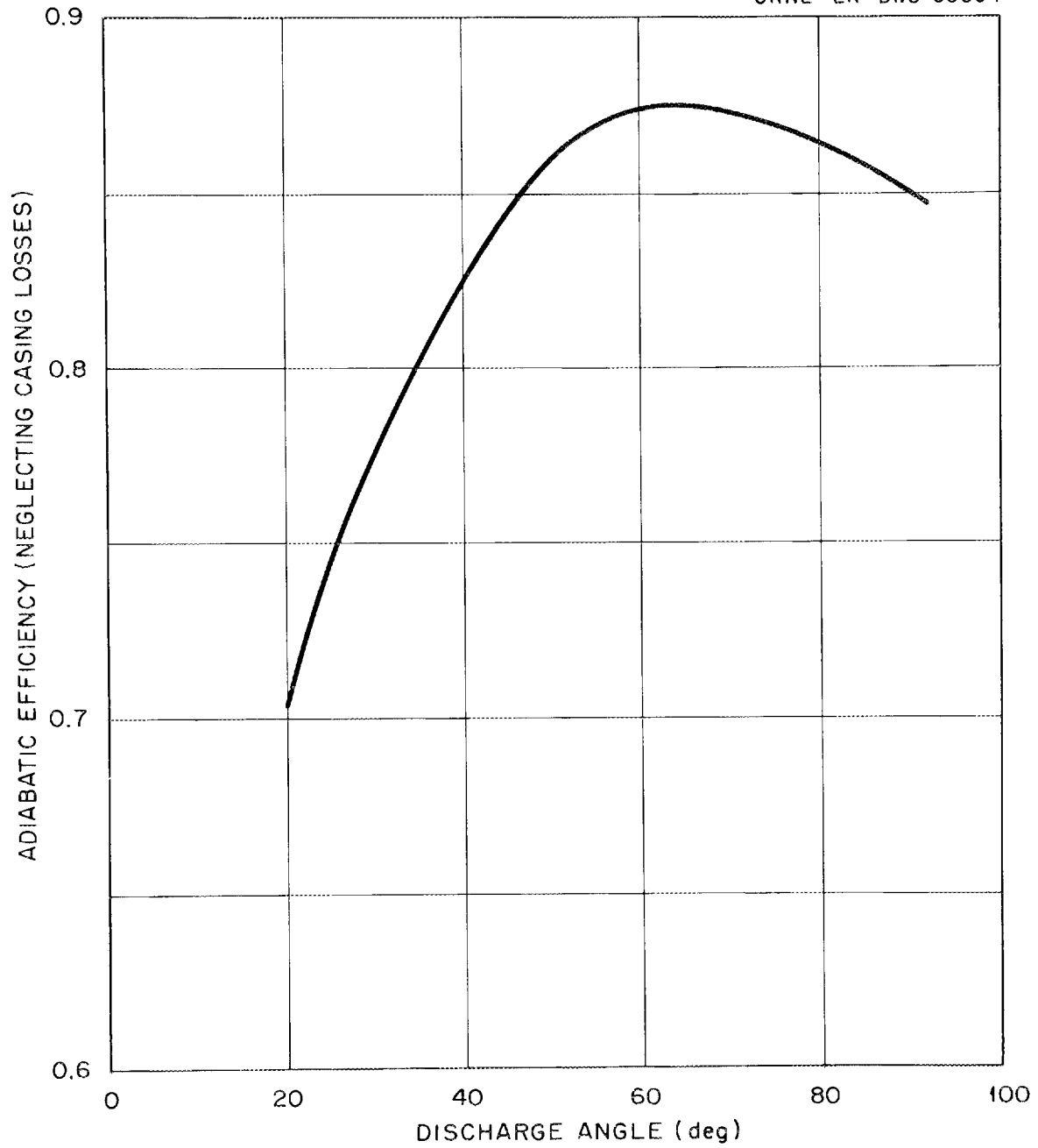
UNCLASSIFIED  
ORNL-LR-DWG 65094

Fig. 4. Efficiency vs Vane Angle at Exit [Baljé (2)].

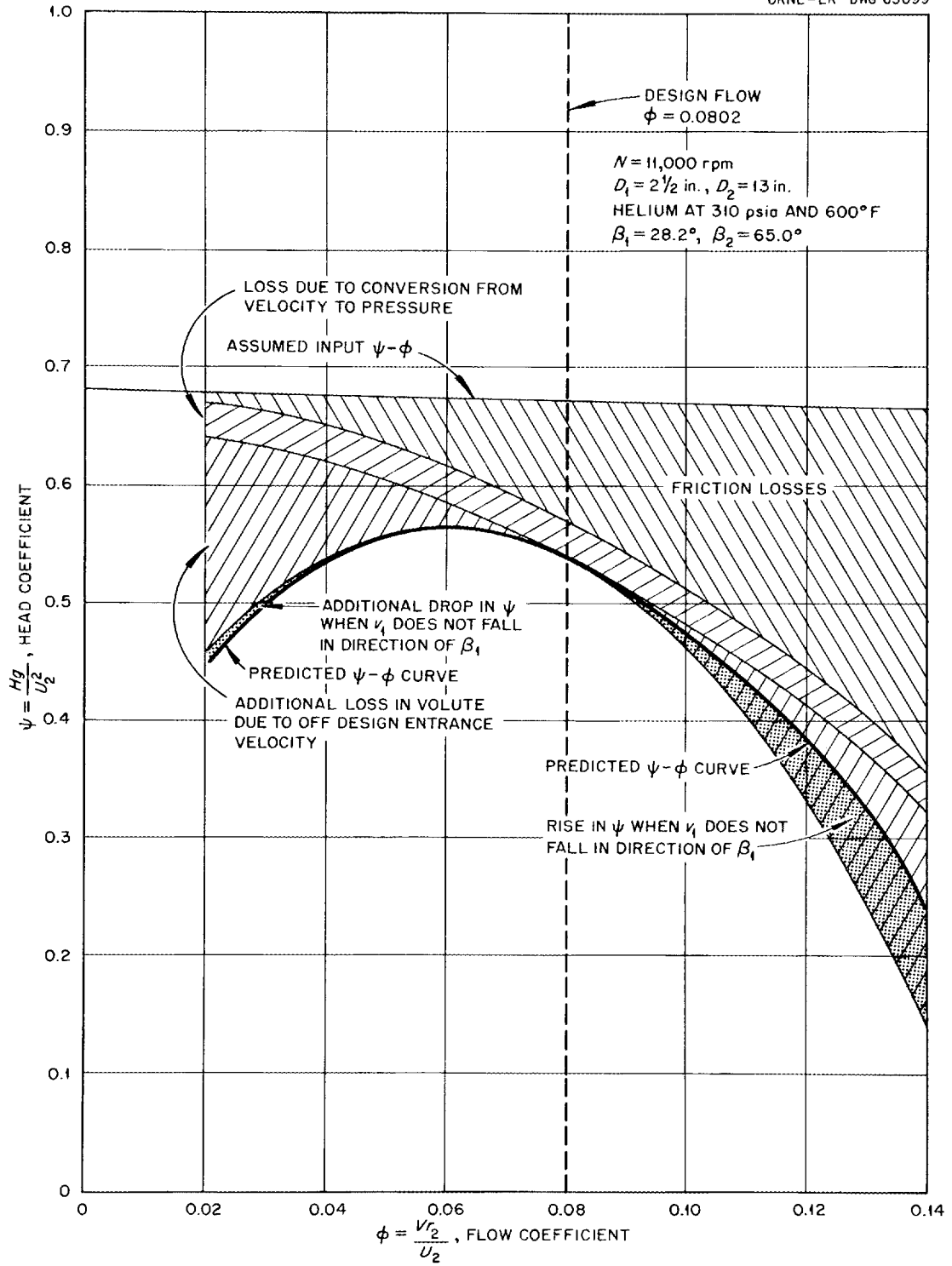


Fig. 5. Head Losses in Centrifugal Compressor.

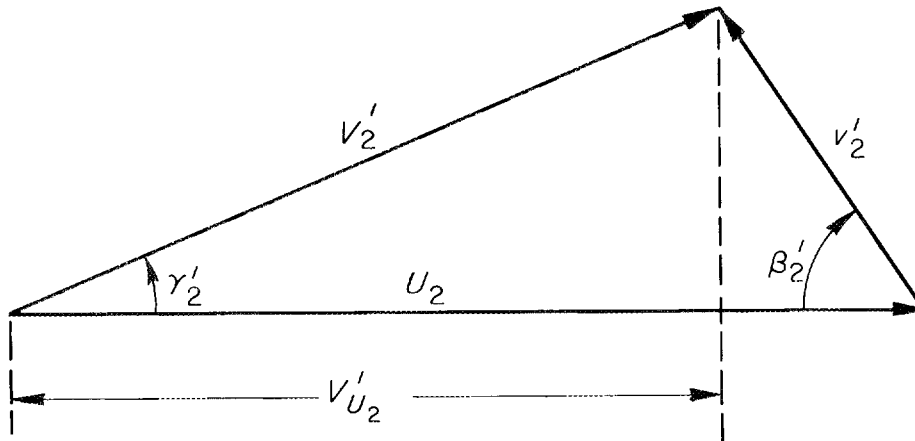
UNCLASSIFIED  
ORNL-LR-DWG 71572

Fig. 6. Fluid Velocity Triangle.

$$H_I = \frac{1}{2g_L} \left( 2U_2V'_2 \cos \gamma'_2 - 2U_1V_1 \cos \gamma_1 \right) . \quad (23)$$

But

$$V'_2 \cos \gamma'_2 = V'_{U_2} \quad (24)$$

and

$$V_1 \cos \gamma_1 = V_{U_1} ; \quad (25)$$

then

$$H_I = \frac{1}{g_L} (U_2V'_{U_2} - U_1V_{U_1}) . \quad (26)$$

Assuming that flow is fully radial at vane inlet

$$V_{U_1} = 0 . \quad (27)$$

Then

$$H_I = \frac{U_2 V_{U_2}}{g_L} \quad (28)$$

Assuming that  $v'_2$  is radial

$$V'_{U_2} = U_2 \quad (29)$$

Then

$$H_I = \frac{U_2^2}{g_L} \quad (30)$$

Let

$$H = H_I \psi \quad (31)$$

Then

$$H = \frac{\psi}{g_L} U_2^2 \quad (32)$$

But

$$U_2 = \frac{D_2 \omega}{2} \quad (32)$$

Therefore

$$H = \frac{\psi}{g_L} \left( \frac{D_2 \omega}{2} \right)^2, \quad (33)$$

which, upon rearrangement, gives the tip diameter:

$$D_2 = \frac{2}{\omega} \left( \frac{Hg_L}{\psi} \right)^{1/2}, \quad (34)$$

where

$\omega$  = angular velocity, rad/sec,

$H$  = head, ft,

$\psi$  = head coefficient, dimensionless,

$g_L$  = acceleration due to gravity = 32.2 ft/sec<sup>2</sup>.

Equation (34) involves only the angular speed, head rise, and experimental head coefficient. Thus, the outside diameter of an impeller can be estimated before the velocity triangles are known. If such an equation were not available, the solution for the exit diameter would involve a trial and error solution that would be time-consuming at best.

The head coefficient can be estimated from Fig. 3. It should be emphasized, however, that Eq. (34) is used merely to estimate the outside diameter. A detailed analysis of the flow through the impeller will be made in succeeding sections. This analysis will show whether the estimated diameter is adequate.

#### Number of Blades Needed

It is far better to have too many blades than to have too few (34). If there are not enough blades, large losses occur because of poor guidance of the fluid. If there are too many blades, friction losses increase slightly. Pfleiderer (23) gives Eq. (35), which is a convenient way to compute the number of vanes required:

$$z = \xi \frac{D_2 + D_1}{D_2 - D_1} \sin \frac{\beta_1 + \beta_2}{2}, \quad (35)$$

where

$$\xi = 10 \sin \frac{\beta_1 + \beta_2}{2},$$

$z$  = number of blades,

$D_2$  = outside diameter,

$D_1$  = inside diameter,  
 $\beta_1$  = inlet vane angle,  
 $\beta_2$  = outlet vane angle.

Normally a machine will have from 10 to 30 blades, depending on its size. In some designs, it is advisable to use secondary vanes, which are sometimes called splitter vanes, in addition to the standard vanes. This subject will be covered in the latter part of this chapter.

#### Slip Between Fluid and Impeller at Outlet

Nichols, McPherson, and Baljé (21) give Eq. (36) with which to compute the slip between impeller and fluid:

$$S = 1 + \frac{1 + 0.6 \sin \beta_2}{0.5z(1 - 0.2833\delta)} \quad , \quad (36)$$

where

$S$  = slip factor = ratio of theoretically possible peripheral component of absolute velocity to actual value,  
 $z$  = number of blades,  
 $\beta_2$  = exit blade angle,  
 $\delta$  = ratio of impeller eye diameter to outer diameter.

#### Outlet Velocity Triangle

The radial component of the exit relative velocity should be somewhat smaller than the inlet velocity ( $V_1$ ) so that some pressure rise will occur due to this component. The impeller guides the fluid somewhat better than does the collector. The following equation is used to calculate the tip velocity of the impeller:

$$U_2 = r_2\omega \quad , \quad (37)$$

where  $r_2$  is the outer radius of the impeller, ft. The theoretical exit relative velocity is indicated in Fig. 7, where

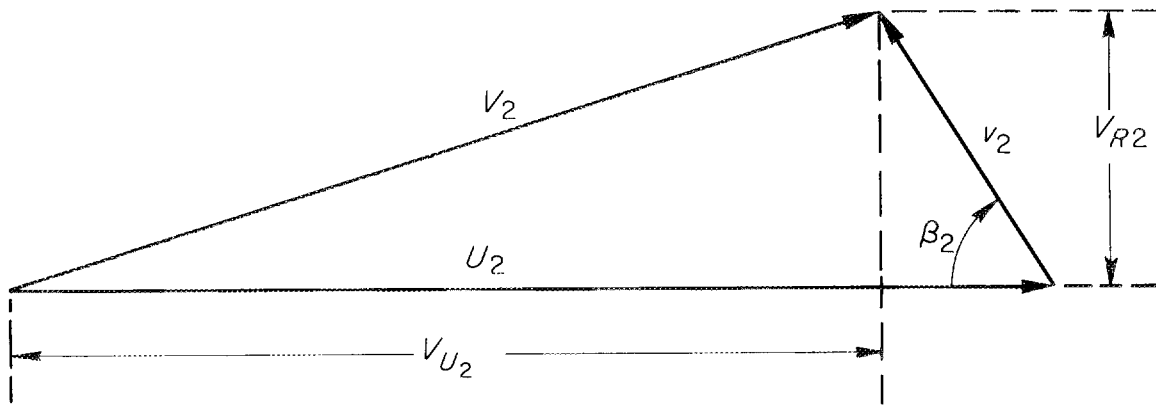
UNCLASSIFIED  
ORNL-LR-DWG 71573

Fig. 7. Theoretical Exit Velocity Triangle.

$$\tan \beta_2 = \frac{V_{R2}}{U_2 - V_{U2}} \rightarrow U_2 - V_{U2} = \frac{V_{R2}}{\tan \beta_2} , \quad (38)$$

and

$$v_2 = \left[ V_{R2}^2 + (U_2 - V_{U2})^2 \right]^{1/2} . \quad (39)$$

The actual fluid absolute velocities at the exit are indicated by the primed letters in Fig. 8. In the preceding section,  $U_2 - V_{U2}$  was calculated. Since  $U_2$  is known,  $V_{U2}$  is easily found. Thus,

$$V'_{U2} = \frac{V_{U2}}{S} , \quad (40)$$

$$V'_2 = \left[ (V_{R2})^2 + (V'_{U2})^2 \right]^{1/2} , \quad (41)$$

$$v'_2 = \left[ (V_{R2})^2 + (U_2 - V'_{U2})^2 \right]^{1/2} , \quad (42)$$

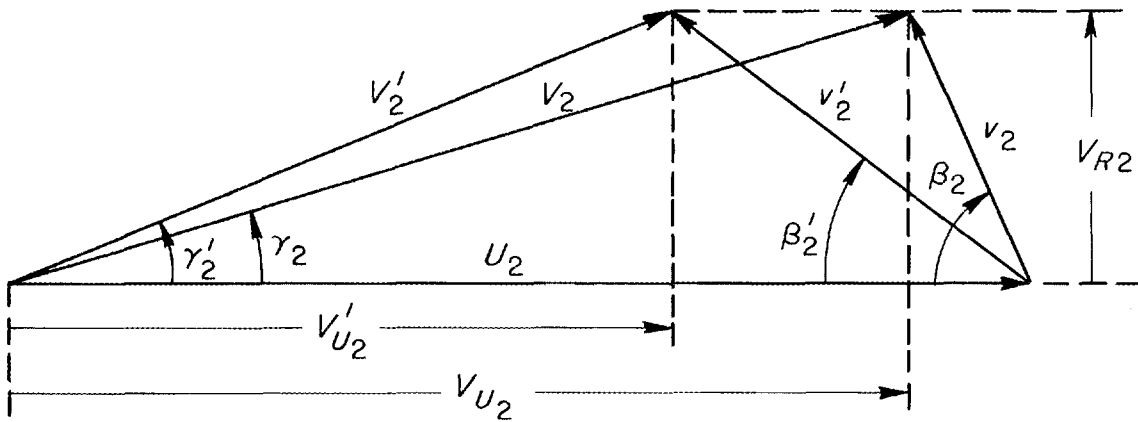


Fig. 8. Actual Exit Velocity Triangle.

and

$$\gamma_2' = \arcsin \frac{V_{R2}}{V_2'} \quad (43)$$

#### Check of Outer Diameter Calculation

The inlet and outlet velocity triangles have at this point been completely described. The approximate outside diameter was computed from Eq. (34), and now it is important that the velocity triangles be used to check this diameter. If the head produced is inadequate, a new diameter is assumed and the exit velocity triangle is recalculated.

This derivation is extremely important in that it points out the three components of pressure rise in a centrifugal compressor. The basic equation is the first law of thermodynamics for steady flow.

The first law of thermodynamics (steady flow),

$$\Delta Q - \Delta W = \Delta H + \Delta kE + \Delta PE \quad , \quad (44)$$

is used to establish the energy balance. Since the fluid is in the impeller only a short time and there are only slight changes in elevation, it is reasonable to assume no transfer of heat and no change in potential energy; that is,

$$\Delta Q = 0, \quad \Delta PE = 0 \quad ,$$

therefore

$$-\Delta W = \Delta H + \Delta kE \quad . \quad (45)$$

The pressure rise due to a change in kinetic energy is

$$\Delta kE = \frac{m}{2g_c} (V_2'^2 - V_1^2) = \frac{m\rho}{2g_c} \Delta pk \quad , \quad (46)$$

where  $\Delta pk$  is the pressure rise due to change in kinetic energy. The pressure rise due to change in enthalpy is

$$\Delta H = m \left( u_2 - u_1 + \frac{p_2}{\rho_2} - \frac{p_1}{\rho_1} \right) \quad . \quad (47)$$

In some instances the temperature rise through the compressor will be quite small. The change in internal energy should also be small; that is,

$$\Delta u \cong 0 \quad .$$

There is often little change in density during the compression (if there is a significant change, a mean value should be used):

$$\rho_2 \cong \rho_1 = \rho \quad .$$

Then

$$\Delta H = \frac{m}{\rho} (p_2 - p_1) \quad . \quad (48)$$

The pressure rise through the compressor is due to the centrifugal field and also due to the change in relative velocity through the vanes (see Fig. 9 for notation). For centrifugal rise, the mass in the element is

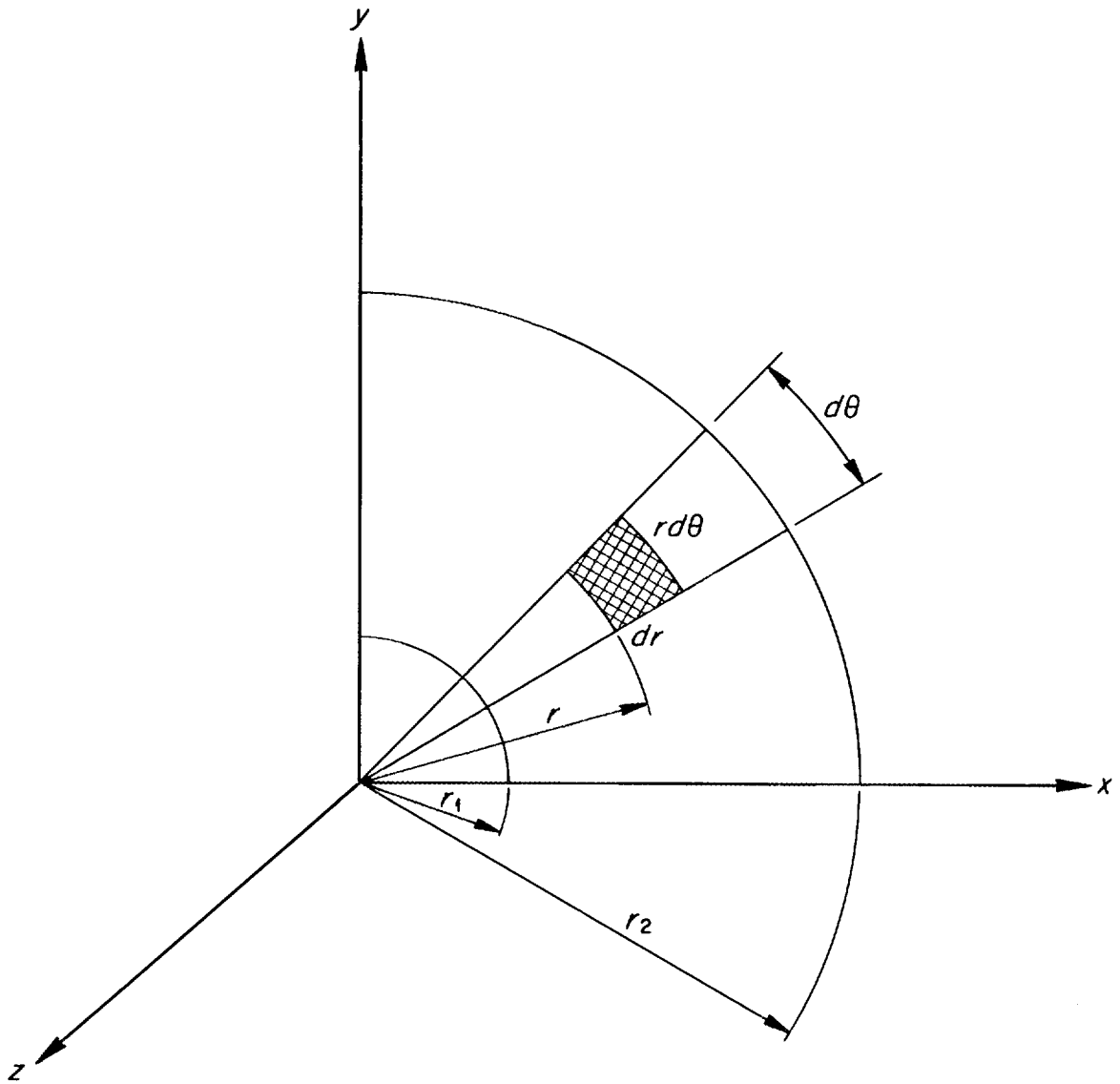


Fig. 9. Fluid Element in Impeller.

$$dm = r \, d\theta \, dr \, dz \, \rho \frac{1}{g_c} , \quad (49)$$

and the centrifugal force on the element is

$$dF_r = \frac{dm}{g_c} r\omega^2 = \frac{dmU^2}{g_c r} , \quad (50)$$

where

$r_2$  = exit radius,

$r_1$  = entrance radius.

The centrifugal force on the element must be balanced by radial pressure on the element:

$$dF_r = P_{r+dr} r d\theta dZ - p_r r d\theta dZ , \quad (51)$$

$$\frac{\rho}{g_c} r d\theta dr dZ \frac{r^2 \omega^2}{r} = p_{r+dr} r d\theta dZ - p_r r d\theta dZ , \quad (52)$$

$$\frac{\rho}{g_c} dr \frac{r^2 \omega^2}{r} = p_{r+dr} - p = dp ,$$

and

$$\Delta p_c = \int_{p_{r_1}}^{p_{r_2}} dp = \frac{\omega^2}{g_c} \int_{r_1}^{r_2} \rho r dr . \quad (53)$$

If  $\rho$  is assumed to be constant, for centrifugal rise

$$\Delta p_c = \frac{\rho}{2g_c} (U_2^2 - U_1^2) , \quad (54)$$

where  $\Delta p_c$  is the pressure rise due to a centrifugal field.

For a rise due to a change in relative velocity,

$$\Delta p_R = \frac{\rho}{2g_c} (v_1^2 - v_2'^2) . \quad (55)$$

The total power absorbed by the fluid is obtained by adding the three components of power:

$$P = \frac{m}{2g_c} \left[ (v_2'^2 - v_1^2) + (U_2^2 - U_1^2) + (v_1^2 - v_2'^2) \right] . \quad (56)$$

Equation (56) gives the power input to the fluid in the impeller. Centrifugal impellers are usually designed so that the first and second terms in Eq. (56) are larger than the third term:

$$H_I = \frac{1}{2g_c} (V_2'^2 - V_1^2 + U_2^2 - U_1^2 + v_1^2 - v_2'^2) \quad (57)$$

This ideal head rise is then multiplied by an appropriate over-all hydraulic efficiency, which is about 80% for a specific speed of 800. This is the actual head rise which can be expected from the machine:

$$H = \eta_o H_I \quad (58)$$

where  $\eta_o$  is the over-all hydraulic efficiency.

#### Impeller Outlet Static Pressure Head and Outlet Static Pressure

The impeller exit static pressure head is calculated with the use of Eq. (59). It may be seen that Eq. (59) consists of the last two terms of Eq. (57). The first term in Eq. (57) is the static head rise in the volute:

$$H_s = \frac{1}{2g_c} (U_2^2 - U_1^2 + v_1^2 - v_2'^2) \quad (59)$$

The corresponding pressure ratio is

$$\frac{p_1}{p_{2s}} = \left( \frac{H_s}{\frac{J T_1 C_p}{g_c} + 1} \right)^{k/(1-k)} \quad (60)$$

Hence

$$p_{2s} = p_1 \left( \frac{H_s}{\frac{J T_1 C_p}{g_c} + 1} \right)^{k/(k-1)} \quad (61)$$

### Impeller Exit Temperature

The temperature rise through the impeller may be calculated in any of several ways. Two methods will be given below which are commonly used by compressor designers. The impeller exit temperature can be calculated from isentropic relationships based on Fig. 10 and the following equation:

$$T_2 = T_1 \left( \frac{p_{2s}}{p_1} \right)^{(k-1)/k} \quad (62)$$

The approximate fluid temperature rise can also be computed from the work of Keenan and Kaye (18). The inlet temperature and pressure are known, as well as the impeller exit pressure ratio. Therefore, the following relationship can be used:

$$p_{R1} = \frac{p_1}{p^*} \quad (63)$$

where  $p^*$  is the reference pressure, and

$$p_{R2s} = \frac{p_{2s}}{p^*} = p_{R1} \frac{p_{2s}}{p_1} \quad (64)$$

UNCLASSIFIED  
ORNL-LR-DWG 71575

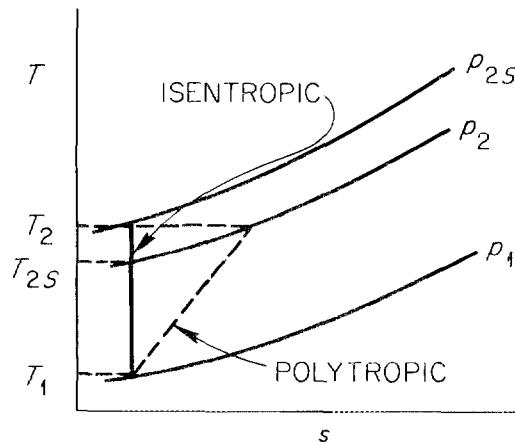


Fig. 10. Compression Process.

Corresponding to  $T_1$  and  $p_1$ , the quantity  $P_{R1}$  is found in the Gas Tables (18) (use table with correct  $k$  value). The pressure ratio  $P_{R2S}$  is then calculated from Eq. (64) and, corresponding to  $P_{R2S}$ ,  $T_2$  is read from the table (18).

The density at the impeller exit is determined from

$$\rho_2 = \frac{P_2}{ZRT_2} , \quad (65)$$

where

$\rho_2$  = impeller exit density,  $\text{lb}_m/\text{ft}^3$ ,

$R$  = gas constant,  $\text{ft}\cdot\text{lb}_f/\text{lb}_m\cdot^\circ\text{R}$ ,

$T_2$  = absolute exit temperature,  $^\circ\text{R}$ ,

$Z$  = compressibility factor,

according to the relations given in Fig. 1.

#### Vane Height at Inlet and Outlet

Inlet. Volume flow through the bladed section includes the leakage shown in Fig. 11. The total mass flow through the impeller is

$$m_T = \lambda m , \quad (66)$$

where

$\lambda$  = leakage factor,

$m$  = through flow mass,

The flow area required is

$$A_1 = \frac{m_T}{\rho_1 V_1} . \quad (67)$$

Part of the inlet cross-sectional area is unavailable for flow because of the vanes. The available area can be calculated as follows:

$$A_1 = \left( \pi D_1 - \frac{z t_1}{\sin \beta_1} \right) h_1 , \quad (68)$$

UNCLASSIFIED  
ORNL-LR-DWG 71576

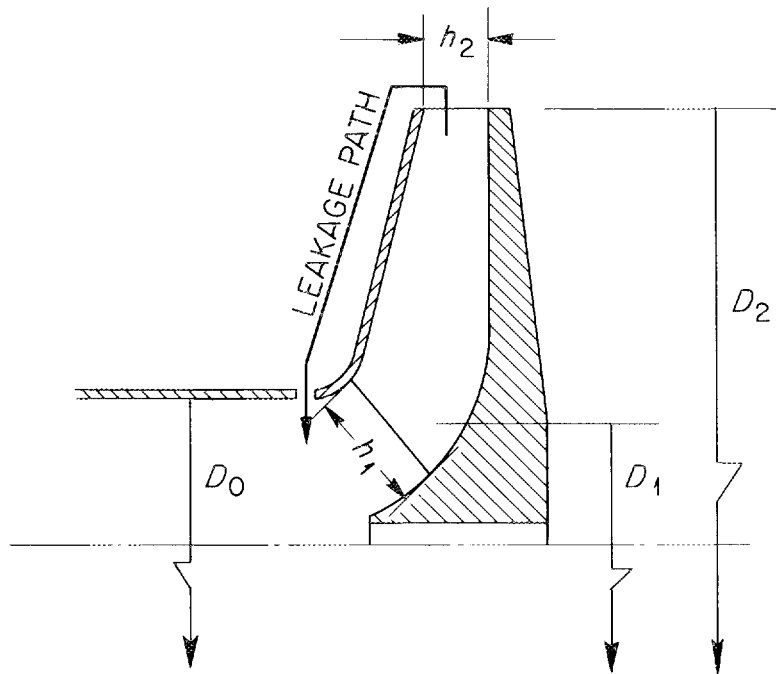


Fig. 11. Impeller Notation.

where

$z$  = number of blades,

$t_1$  = blade thickness at inlet.

Therefore

$$h_1 = \frac{A_1}{\pi D_1 - \frac{z t_1}{\sin \beta_1}} \quad (69)$$

Outlet. The required flow area at the exit from the impeller is

$$A_2 = \frac{m_T}{\rho_2 V_{R2}} \quad (70)$$

The available area is calculated from the following equation:

$$A_2 = \left( \pi D_2 - \frac{z t_2}{\sin \beta_2} \right) , \quad (71)$$

where  $t_2$  is the blade thickness at the exit. Therefore

$$h_2 = \frac{A_2}{\pi D_2 - \frac{z t_2}{\sin \beta_2}} . \quad (72)$$

If splitter vanes are added,  $h_2$  must be changed, since there will be more vanes at the exit that tend to reduce the flow area.

#### Velocity Distribution Along Driving Face of Vanes

In this section a method will be derived to compute the fluid velocity at any point on the leading edge of an impeller vane. In some cases it is wise to add a set of secondary vanes to the impeller when adverse velocity gradients are expected, that is, when the velocity on driving face goes to zero. When the driving face velocity goes to zero, eddies appear and efficiency drops.

The basic equation is given by Stanitz and Ellis (29):

$$\frac{T}{T_0} = 1 + \frac{k-1}{2} [(RM_T)^2 - Q^2] , \quad (73)$$

where

$$R = \frac{r}{r_t},$$

$r_t$  = tip radius,

$T$  = absolute static temperature,

$T_0$  = absolute stagnation temperature,

$k$  = specific head ratio,

$$M_T = \frac{u}{C_0} = \frac{\omega r_t \sin \frac{\alpha}{2}}{C_0} ,$$

$C_o$  = stagnation speed of sound upstream of impeller,

$\omega$  = angular speed,

$$Q = \frac{q}{C_o},$$

$q = (u^2 + v^2)^{1/2}$  = velocity of fluid relative to blades,

$u$  = tangential component of  $q$ ,

$v$  = radial component of  $q$ ,

$\alpha$  = cone angle (see Fig. 12).

By limiting the argument to radial-flow impellers only, the following equations can be written:

$$\alpha = \pi \rightarrow \sin \frac{\alpha}{2} = 1 .$$

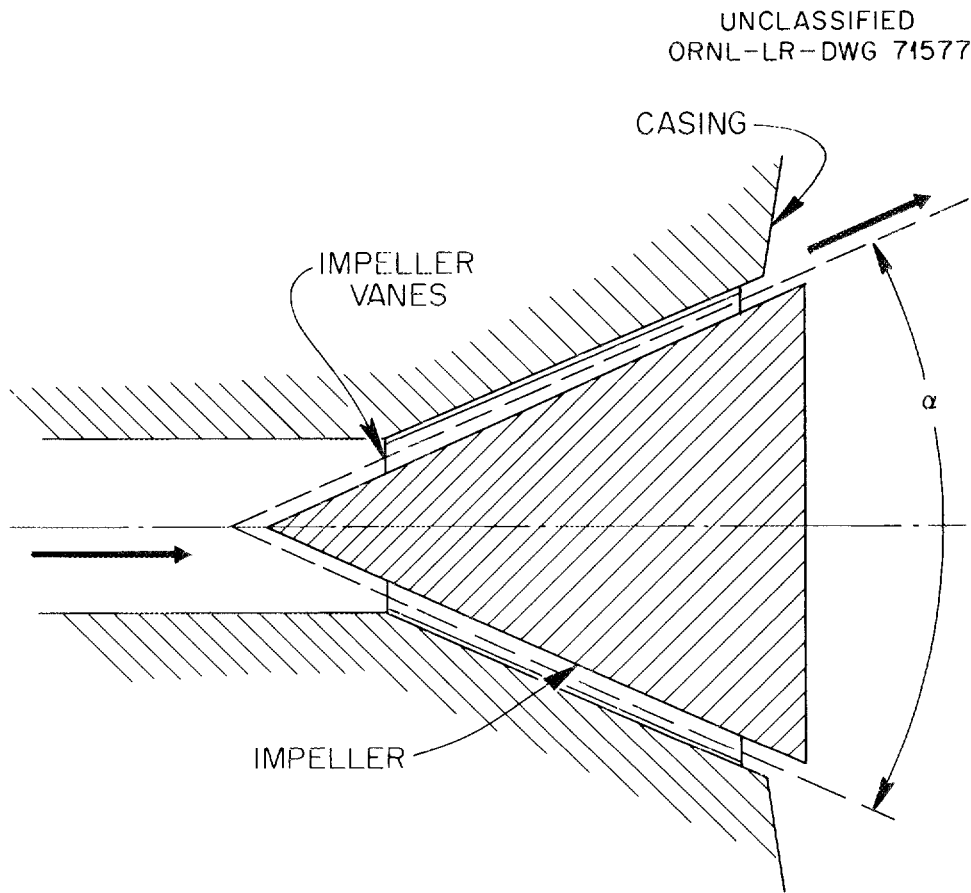


Fig. 12. Impeller Cone Angle.

Therefore

$$M_T = \frac{\omega r_t}{C_o} , \quad (74)$$

$$RM_T = \frac{r}{r_t} \frac{\omega r_t}{C_o} , \quad (75)$$

$$RM_T = \frac{r\omega}{C_o} , \quad (76)$$

or

$$RM_t = \frac{u}{C_o} .$$

Then

$$\frac{T}{T_o} = 1 + \frac{k-1}{2} \left( \frac{u^2}{C_o^2} - Q^2 \right) . \quad (77)$$

Replacing  $Q$  by  $q/C_o$  and factoring out  $1/C_o^2$  then gives

$$\frac{T}{T_o} = 1 + \frac{k-1}{2C_o^2} (u^2 - q^2) . \quad (78)$$

Solving for  $q$ ,

$$q^2 = u^2 + \frac{2C_o^2}{k-1} \left( 1 - \frac{T}{T_o} \right) ,$$

but

$$\frac{T}{T_o} = \left( \frac{p}{p_o} \right)^{(k-1)/k} , \quad (79)$$

where

$p$  = static pressure,

$p_o$  = stagnation pressure upstream of impeller.

Therefore

$$q^2 = u^2 + \frac{2C_o^2}{k-1} \left[ 1 - \left( \frac{p}{p_o} \right)^{(k-1)/k} \right] \quad (80)$$

and

$$q_d^2 = u^2 + \frac{2C_o^2}{k-1} \left[ 1 - \left( \frac{p_d}{p_o} \right)^{(k-1)/k} \right], \quad (81)$$

where

$p_d$  = driving face pressure at any radial location,

$q_d$  = fluid relative velocity on driving face at any radial location.

Introducing

$p_a$  = average pressure in flow channel between two vanes at any radial location,

$\Delta p$  = pressure difference across flow channel at any radial location  
(driving face pressure minus trailing face pressure),

then gives

$$p_d = p_a + \frac{\Delta p}{2} \quad (82)$$

and

$$\frac{p_d}{p_o} = \frac{p_a}{p_o} + \frac{\Delta p}{2p_o} \quad (83)$$

Substituting Eq. (83) into Eq. (81) gives

$$q_d = \left\{ u^2 + \frac{2C_o^2}{k-1} \left[ 1 - \left( \frac{p_a}{p_o} + \frac{\Delta p}{2p_o} \right)^{(k-1)/k} \right] \right\}^{1/2} \quad (84)$$

In order to use Eq. (84), it is necessary to estimate  $p_a$  and  $\Delta p$  along any radius in the impeller. The following method is approximate, but it is felt that for the problem being investigated sufficient accuracy is obtained. If it is assumed that  $p_a$  varies in a linear fashion with radius between  $p_{a1}$  at the impeller inlet and  $p_{a2}$  at the impeller outlet, the data of Hamrick (14) show that the assumption is valid at maximum efficiency which is, of course, the design point. Then

$$p_a = p_{a1} + \frac{p_{a2} - p_{a1}}{r_2 - r_1} (r - r_1) \quad , \quad (85)$$

where

- $p_{a1}$  = average pressure in channel at inlet,
- $p_{a2}$  = average pressure in channel at outlet,
- $r_1$  = inlet radius,
- $r_2$  = outlet radius.

Pressure  $p_a$  and radius  $r$  are the dependent and independent variables, respectively.

From the section on impeller design, isentropic and actual power input to the fluid are known. Thus,

$$P = \tau\omega \rightarrow \tau = \frac{P}{\omega} \quad , \quad (86)$$

where

- $P$  = actual power input to fluid,
- $\tau$  = torque on impeller,
- $\omega$  = impeller angular speed,

and

$$\tau = F_\theta \bar{r} \rightarrow F_\theta = \frac{\tau}{\bar{r}} \quad , \quad (87)$$

where  $F_\theta$  is the resultant equivalent force acting on impeller and  $\bar{r} = (r_1 + r_2)/2$  is the average vane radius. Then

$$F_{\theta N} = \frac{F_{\theta}}{z} , \quad (88)$$

where  $z$  is the number of vanes.

The approximate radial area component for one blade can be found from the relation

$$A_r \cong \left( \frac{h_2 + h_1}{2} \right) (r_2 - r_1) , \quad (89)$$

where

$A_r$  = radial component of blade area,

$h_1$  = blade height at entrance,

$h_2$  = blade height at exit.

The pressure difference across the flow channel is then found by use of the following equation:

$$\Delta p = \frac{F_{\theta N}}{A_r} , \quad (90)$$

which is used in Eq. 84. This method implies that the pressure difference across the flow channel is the same at any radius. This is approximately true for design flow conditions (14).

### Impeller Layout

The most tedious and time-consuming task is that of using the results of the previous computations as a guide to design of the impeller. As the impeller begins to take shape, changes will probably have to be made in the design variables. It is imperative that there be a smooth transition from axial to radial flow at the inlet, that the blade entrance diameter be in correct proportion to the inlet pipe diameter, and that the impeller hub be large enough to accommodate the shaft. If these conditions are not met, additional losses will occur at the inlet.

A layout of an impeller is shown in Fig. 13. No attempt will be made to show detailed drawings of the impeller, since to do so would be to



deviate from the goal of this work which is to design the impeller flow channels. The impeller shown has both primary and secondary vanes. Also, it is apparent that the driving face of the blade is made on one radius and the trailing face is drawn on a different radius.

The following steps are taken to define a blade:

1. From point (1) on  $D_1$  set off angles  $\beta_1$  and  $\beta_2$ . They are measured as shown in Fig. 13.
2. Mark off distance between points (1) and (2) equal to radius  $r_2$ .
3. Draw line between C and (3) bisecting line between (2) and (0) at right angles.
4. Point C is located at the intersection of the line between (1) and C and the line between (3) and C.
5. The driving face of the blade is then drawn with radius  $r_3$  and center C.
6. The blade thicknesses at the inlet and the outlet are then chosen ( $t_1$  and  $t_2$ ).
7. Center  $C'$  is located by trial and error.
8. Once  $C'$  and  $r_4$  are determined, the trailing face of the blades is drawn.
9. The inlet tip of the blade is rounded off.

When one blade has been completely defined, circles are drawn through C and  $C'$  with radii  $r_5$  and  $r_6$ , respectively. It is then quite simple to locate the centers of all of the other blades, since they must fall on these circles.

### 3. CASING DESIGN

The casing of a compressor normally provides a transition from an inlet pipe to an impeller inlet, some type of collector, a diffuser, bearing supports, bearing-lubricant passages, and any number of other necessary services. Since this paper is intended to deal strictly with aerodynamic and thermodynamic design of centrifugal compressors, the word casing will be used to denote those parts of the compressor which direct the working fluid before and after it passes through the impeller.

The inlet section of the casing has the important job of preparing the fluid to enter the impeller. This may involve straightening the flow or increasing or decreasing the fluid velocity or both. After the fluid has passed through the impeller, it must be collected by a volute (also called scroll) and finally passed through a diffuser where its velocity is decreased and its pressure increased. It is most important to keep in mind throughout this discussion that energy is added to fluid only in the impeller. The casing can only change velocity energy into pressure energy or vice versa.

The following pages give steps to be taken in designing a volute and a diffuser, and Fig. 14 explains the notation used.

#### Volute Design

##### Volute Tongue Diameter

Stepanoff (32) has given an empirical equation for estimating the volute tongue diameter:

$$D_3 = 1.15 D_2 \quad , \quad (91)$$

where  $D_3$  is the diameter of the circle through the volute tongue and  $D_2$  is the outer impeller diameter.

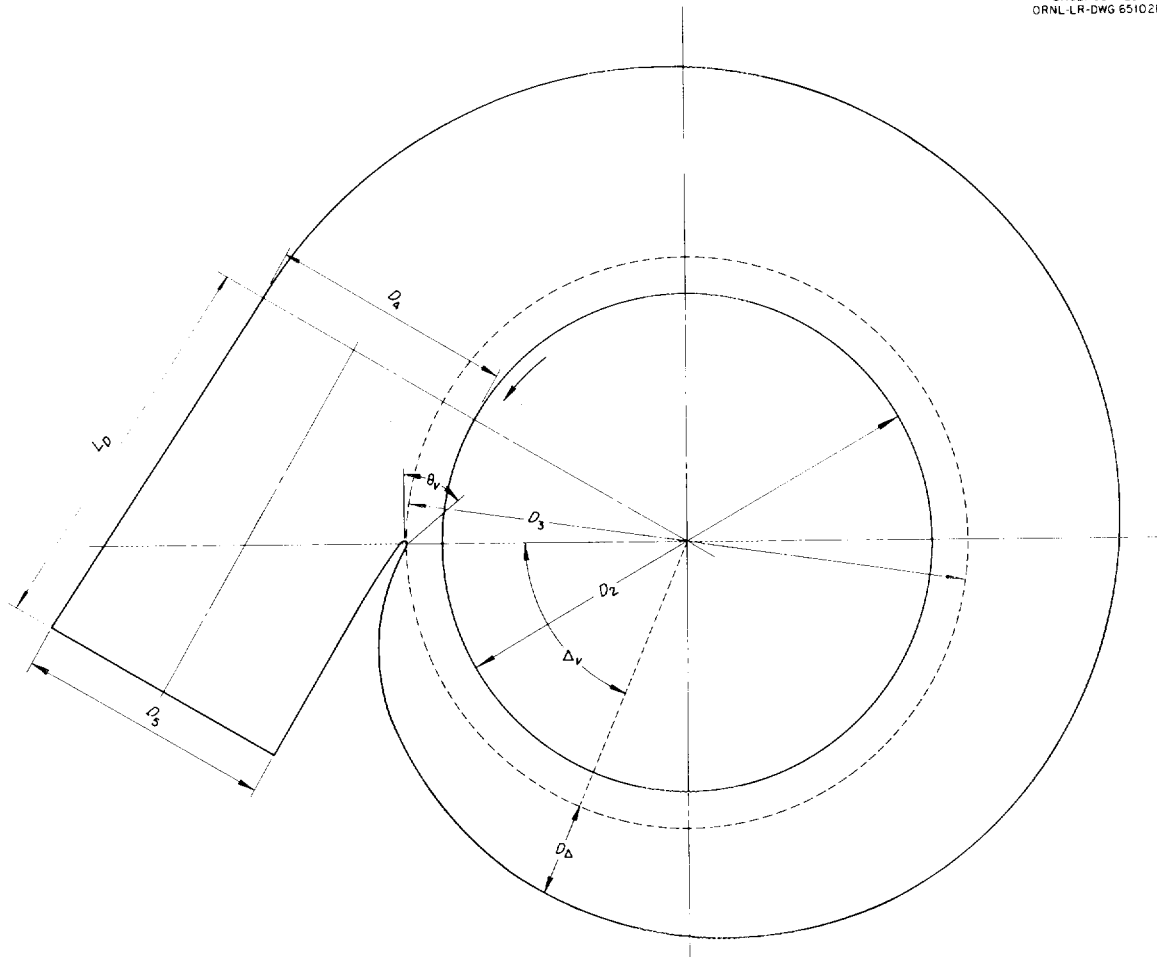


Fig. 14. Casing Notation.

### Average Casing Velocity

The average casing velocity is given by

$$V_v = \sigma V_2' \quad , \quad (92)$$

where  $V_v$  is the average casing velocity,  $\sigma$  is the velocity distribution factor that depends upon the fluid discharge angle, and  $V_2'$  is the absolute fluid velocity at the impeller exit. The velocity distribution factor  $\sigma$  is determined experimentally and is plotted versus impeller discharge angle  $\gamma_2'$ , as in Fig. 15. It is a universal curve that can be used for any gas.

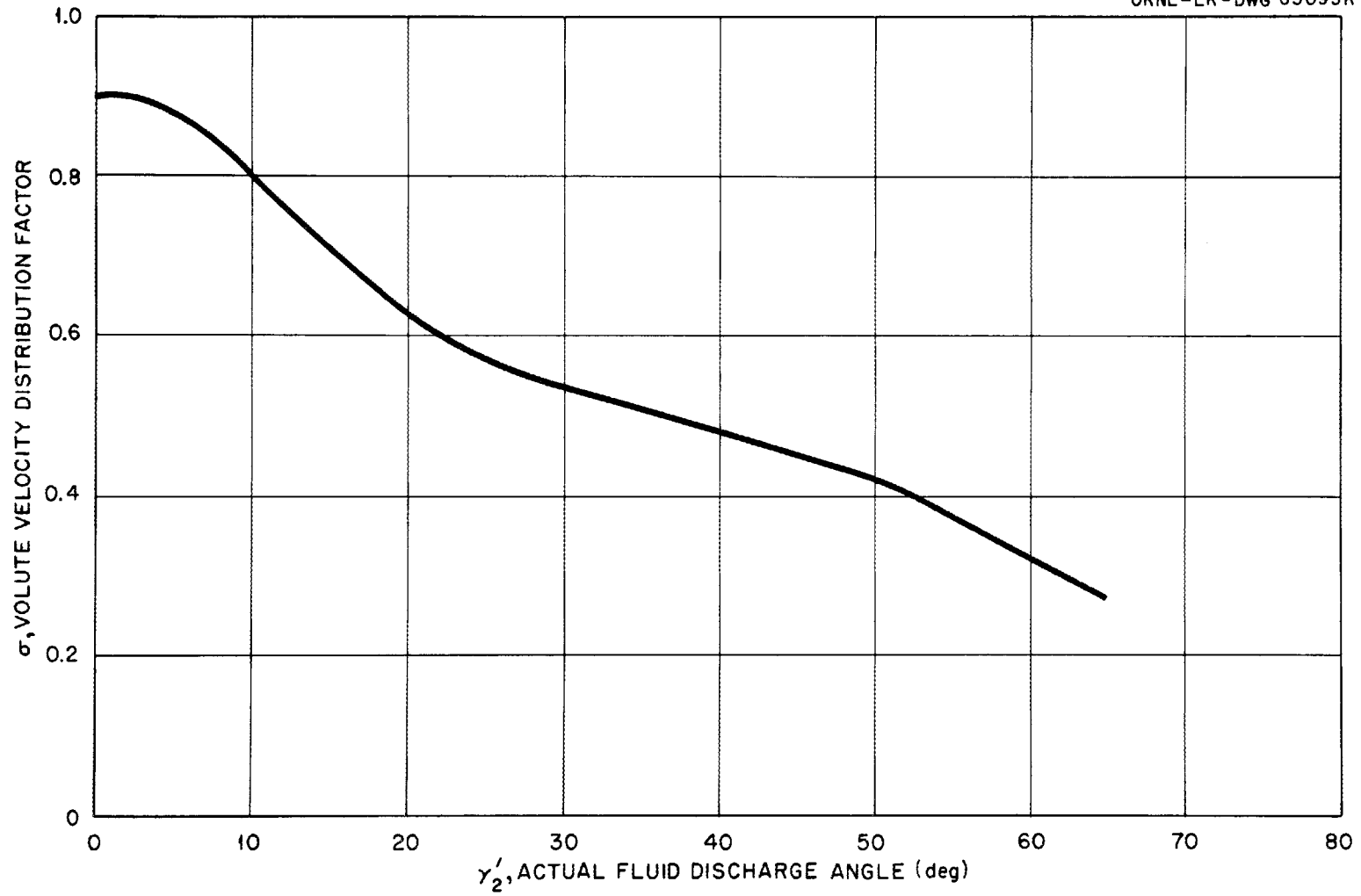


Fig. 15. Volute Velocity Distribution Factor [Stepanoff (32)].

### Volute Outlet Area and Diffuser Inlet Area

Because the average volute velocity is smaller than the average impeller exit velocity, volume flow through the volute will be somewhat smaller than that at impeller exit. The change in velocity is due primarily to the fact that (1) the leakage flow must go through the impeller but it does not go through the volute, and (2) there is a change in density as the fluid leaves the impeller and enters the volute, that is, it is diffused. Before the volute outlet area can be computed, the volume flow through the outlet area must be determined. The mass flow at the volute exit is, of course, the same as the mass flow at the entrance to the compressor.

### Static Pressure and Temperature in the Volute

The static pressure head can be calculated from the static pressure at the impeller exit by the following equation, which is a form of Eq. (57):

$$H_v = \left[ H_s + \frac{1}{2g_c} (v_2'^2 - v_v^2) \right] \eta_0 \quad (93)$$

The pressure and temperature in the volute can then be found from Eqs. (94) and (95). Equation (94) comes from Eq. (12) with  $p_v$  and  $H_v$  in place of  $H$  and  $p_2$ :

$$p_v = p_1 \left[ \frac{H_v}{J T_1 C_p \left( \frac{g_c}{g_L} \right)} + 1 \right]^{k/(k-1)} \quad (94)$$

$$T_v = T_1 \left( \frac{p_v}{p_1} \right)^{(k-1)/k} \quad (95)$$

The average density in the volute is given by

$$\rho_v = \frac{p_v}{ZRT_v} , \quad (96)$$

and the volume flow at volute outlet is

$$Q_4 = \frac{\dot{m}}{\rho_v} . \quad (97)$$

The required volute outlet area, that is, the area normal to the fluid flow, is

$$A_4 = \frac{Q_4}{V_v} . \quad (98)$$

The cross-sectional area required at several intermediate angles between the tongue ( $\Delta_v = 0$ ) and the volute outlet ( $\Delta_v = 2\pi$ ) is then determined from the relation

$$A_\Delta = A_4 \frac{\Delta}{2\pi} , \quad (99)$$

where  $A_\Delta$  is the area required at angle  $\Delta$ , and  $\Delta_v$  is the angle measured from the volute tongue. The volute tongue angle is

$$\theta_v = \gamma_2' ,$$

where  $\theta_v$  is the volute tongue angle shown in Fig. 14, and  $\gamma_2'$  is the angle between the fluid and the tangent to the impeller at the exit from the impeller.

The design procedure given above should ensure that the average velocity is approximately the same in all cross sections of the volute. The static pressure should also be approximately constant around the periphery of the impeller. It has been found experimentally that such a velocity and pressure distribution gives the best efficiency (32). These conditions hold only at the design point. Off-design conditions will be discussed in the section on transient operation of compressors.

At no point in this analysis has the shape of the volute cross section been fixed. Changes in volute geometry and surface conditions in general produce only slight effects on compressor performance. A thorough discussion of volute geometry is given by Brown and Bradshaw (7).

### Diffuser Design

#### Diffuser Angle

The total included angle,  $\theta_D$ , should be between 8 and 10 degrees (see Fig. 16). This gives very good efficiency, as shown in Fig. 17.

#### Inlet and Outlet Areas for Diffuser

The inlet area is, of course, the same as the volute exit area ( $A_4$ ). The exit area depends on several factors. In some cases it is desirable to have the same size piping throughout the system. To meet this requirement the area,  $A_5$ , should be the same as the piping inside area. In other instances, the exit velocity is the important factor. For example, high velocities might be required in order to achieve good heat transfer when

UNCLASSIFIED  
ORNL-LR-DWG 71578

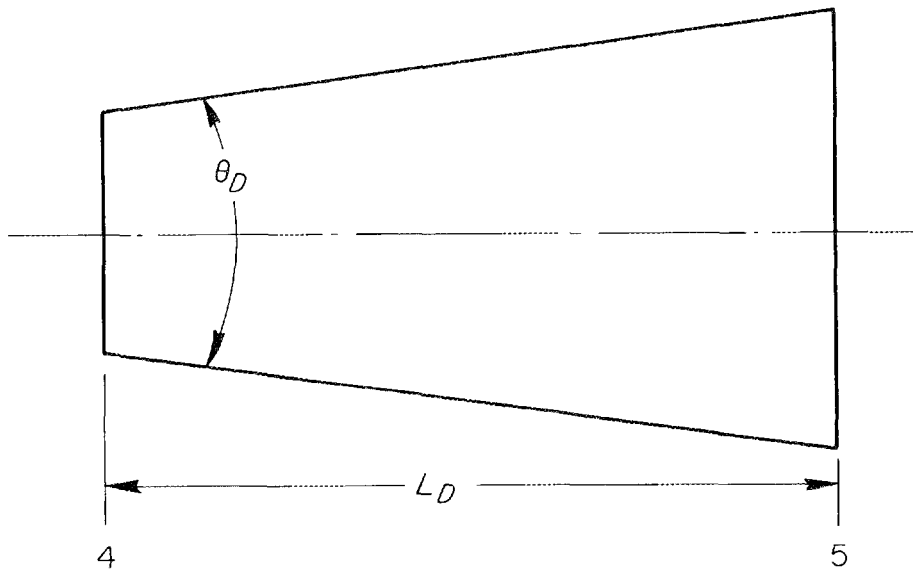


Fig. 16. Diffuser Notation.

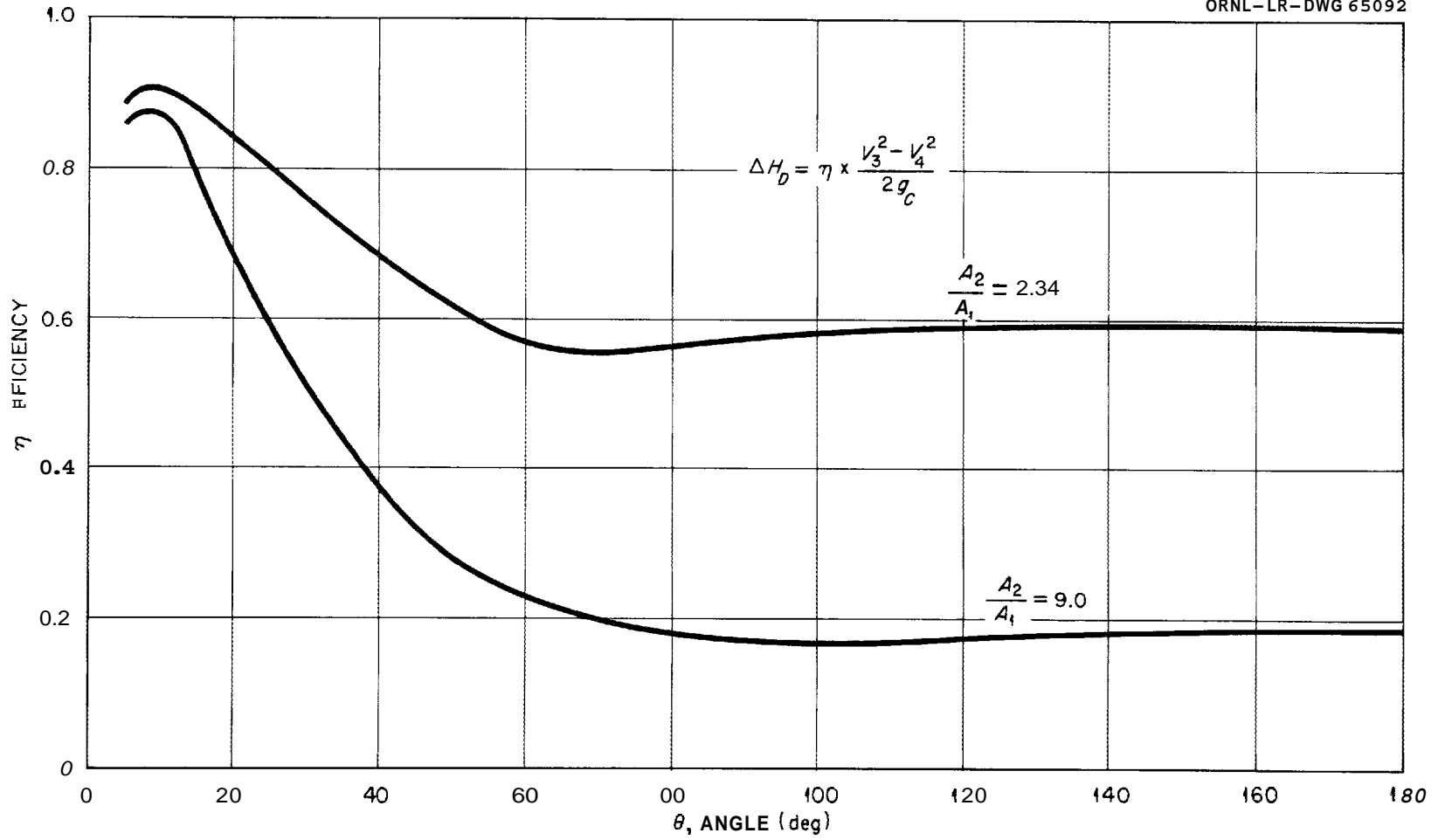


Fig. 17. Conical Diffuser Efficiency vs Total Included Angle [Binder (5)].

the compressor exhaust gas is to be cooled. The exit area would then be chosen to give the desired velocity.

Length of the Diffuser ( $L_D$ )

Once the divergence angle and inlet and outlet areas have been fixed, the diffuser is completely defined. The length is easily found from these characteristics and the following equation:

$$L_D = \frac{D_5 - D_4}{2 \tan\left(\frac{\theta_D}{2}\right)} \quad (100)$$

#### 4. PREDICTION OF HEAD-FLOW CURVES

At the present time there is considerable lack of knowledge concerning boundary-layer behavior within the passages of centrifugal compressors. It is therefore difficult to predict with any degree of accuracy the actual output head and flow characteristics of a particular machine. Many investigators have worked on this subject, but at present it appears that none of the existing methods can be used with complete satisfaction over the range of application of centrifugal compressors. It is hoped that, in the future, as more is learned of the flow within centrifugal compressors, a method can be developed for predicting the output head and flow behavior of a proposed design.

Although there is no exact means with which to predict compressor performance, it is imperative in some cases to have at least an estimate before a machine is built. Several reports of estimating methods have been reviewed. Kovats (19) reported the interesting and informative treatment of the subject that is the basis for the following work. The method illustrated below is not the same as that given by Kovats, the difference being primarily the substitution of Stepanoff's  $\psi - \phi$  curve for the input head curve. In Stepanoff's curve  $\phi = Vr_2/U_2$ , the flow coefficient, and  $\psi = H_g/U_2^2$ , the head coefficient. All loss coefficients and other experimental data were taken from Kovats' work.

A typical head-flow curve was shown above in Fig. 5, with all the losses shown, as well as the input head-flow curve. As may be seen, the various losses change with change in flow rate. The methods for estimating those losses are described below.

##### Outline of Method

An input head-flow curve is assumed and the various losses are subtracted from it. These losses are termed: friction loss, loss of conversion from velocity to pressure, volute loss, and entrance loss. Equations are given that can be used to estimate these losses.

### Friction Losses

The impeller inlet velocity components, in polar coordinates, are shown in Fig. 18. The friction at any desired point is given by

$$\left(\frac{h_f}{H_i}\right)_f = \frac{h_f}{H_i} \left(\frac{W_{\infty X}}{W_{\infty}}\right)^2, \quad (101)$$

where

$$W_{\infty} = \left[ \left( \frac{v_{1\theta} + v_{2\theta}}{2} \right)^2 + \left( \frac{v_{1r} + v_{2r}}{2} \right)^2 \right]^{1/2}, \quad (102)$$

= vectoral average between relative velocity at inlet and outlet,

$v_{\theta}$  = peripheral component of relative velocity,

$v_r$  = normal component of relative velocity,

$\frac{h_f}{H_i}$  = friction at design point,

$h_f$  = frictional head loss at design point,

$H_i$  = input head at design point,

UNCLASSIFIED  
ORNL-LR-DWG 71579

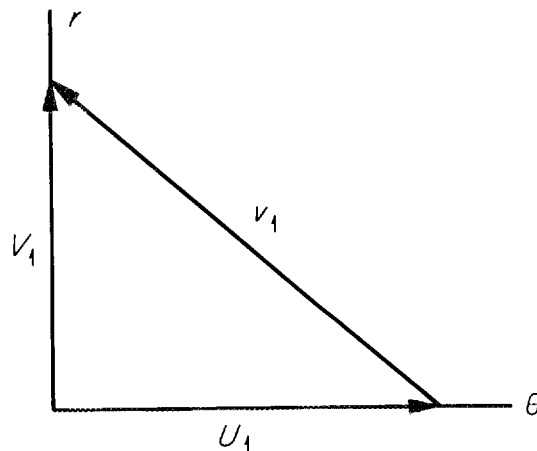


Fig. 18. Impeller Inlet Velocity Components in Polar Coordinates.

$$x = \frac{\psi_{ix}}{\psi_i} ,$$

$\psi_{ix}$  = input head coefficient at any point on input characteristic curve,

$\psi_i$  = input head coefficient at design flow.

The head loss from friction is proportional to the square of velocity head of average relative velocity ( $W_\infty$ ). This is immediately apparent from Eq. (101). Computing time can be considerably reduced if  $(W_{\infty x}/W_\infty)^2$  in Eq. (101) is replaced by  $(\phi_x/\phi)^2$ . This substitution in most situations should introduce only slight errors, since as flow is changed in a centrifugal compressor the inlet relative velocity changes about the same percentage as does the exit relative velocity.

The friction head loss ratio  $(h_f/H_i)_f$  ranges from 0.04 to 0.10. The lower the value of  $K_f$  the higher the value of  $H_f/H_i$ , where

$$K_f = \frac{Q}{r_2 U_2} ,$$

which is the Rateau flow coefficient, and  $Q$  is the volume flow rate.

#### Loss of Conversion from Velocity to Pressure

In determining the loss of conversion at the design point from velocity to pressure, it is assumed that

$$\frac{h_c}{H_i} = \text{constant},$$

where  $h_c$  is the conversion head loss. In most all machines with a volute, the conversion loss is nearly zero in the impeller, since it is designed so that very little conversion occurs in the impeller. In the volute, the ratio  $h_c/H_i$  is between 0.02 and 0.03. If a vaned diffuser is used,  $h_c/H_i$  can be as high as 0.05. When a volute is used  $h_c/H_i$  can be approximated as follows:

$$\frac{h_c}{H_i} = 0.025 . \quad (103)$$

### Additional Loss in the Volute

There is an additional conversion loss in the volute at off-design conditions. Volute can be designed to perform at maximum efficiency only for one flow condition (the design point). For any other flow conditions the following additional losses are encountered:

$$\frac{h_d}{H_i}_x = 0.4 \psi_i \left[ x - 1 + \epsilon \left( 1 - \frac{\phi_x}{\phi} \right) \right]^2, \quad (104)$$

where  $\epsilon$  is the ratio of the radius at the outlet of the impeller to the radius to the center of the 360° volute section, and  $h_d$  is the additional head loss in the volute at off-design flows.

### Entrance Loss

An entrance loss occurs at off-design conditions because the fluid does not enter the impeller vanes in the direction of the blade angle (see Fig. 19). This loss may be expressed by

$$\frac{h_e}{H_i}_x = \frac{1}{2\psi_i} \left( \frac{v_1 \phi_x}{U_2 \phi} \right)^2 \sin \Delta\beta_{1x}, \quad (105)$$

where

$\Delta\beta_{1x}$  = angle between  $\beta_1$  and  $\beta_{1x}$ ,

$\beta_1$  = vane inlet angle,

$\beta_{1x}$  = fluid inlet angle.

From data given by Hamrick (14),  $\Delta\beta_{1x}$  can be estimated to vary in a linear fashion from +15° (low flow near shutoff) to -15° (high flow near maximum capacity).

### Output Head Coefficient

If the losses are now subtracted from the input head coefficient at corresponding flows, the actual  $\psi - \phi$  characteristic curve will be obtained.

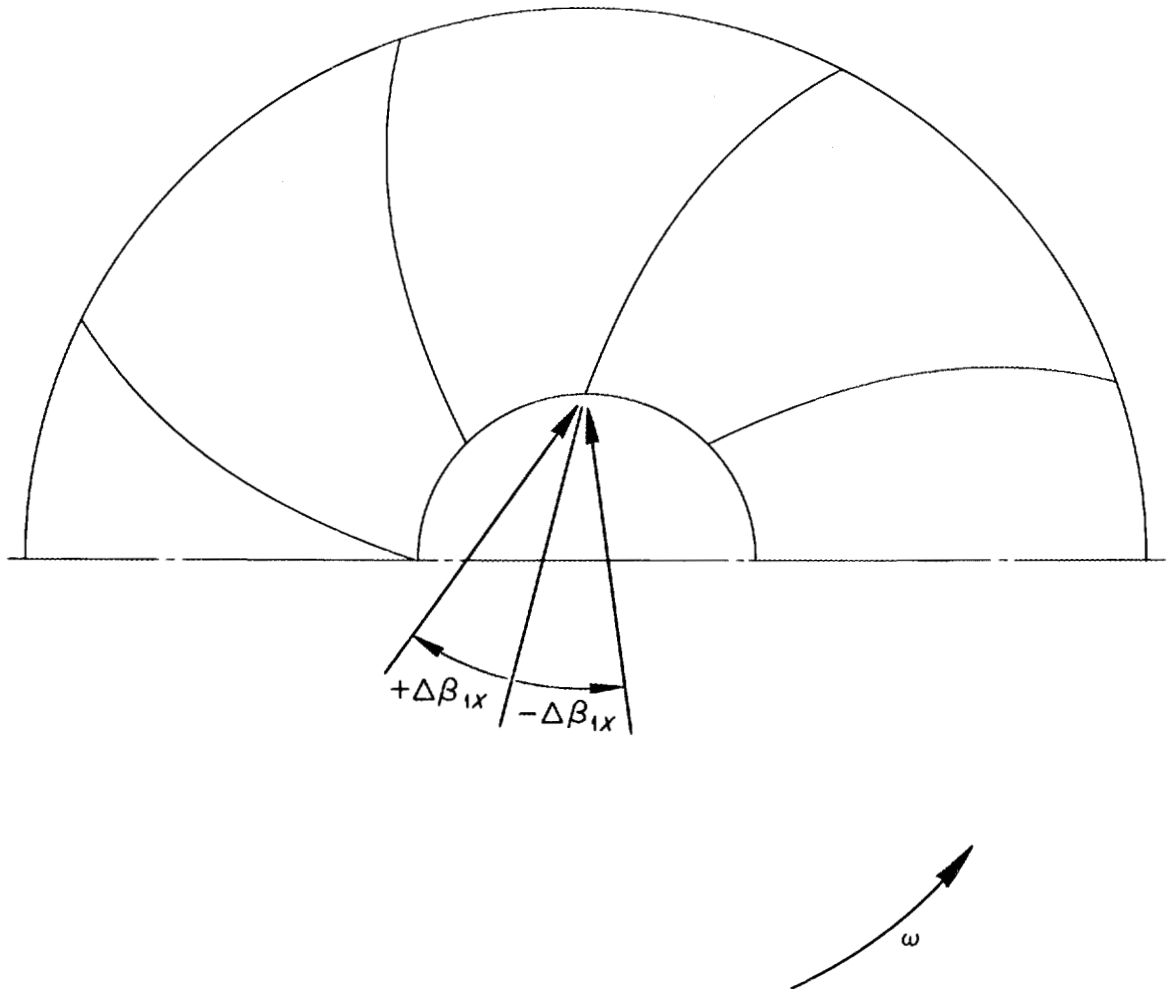


Fig. 19. Change in Relative Inlet Angle at Off-Design Flows.

It is then quite easy to find the head-flow curve for the compressor in question. The head coefficient is

$$\psi_x = \psi_{ix} - \frac{h_f}{H_i} \left( \frac{\phi_x}{\phi} \right)^2 - 0.4\psi_i \left[ x - 1 + \epsilon \left( 1 - \frac{\phi_x}{\phi} \right) \right]^2 - \frac{1}{2\psi_i} \left( \frac{v_1 \phi_x}{U_2 \phi} \right)^2 \sin \Delta\beta_{1x} - \frac{h_c}{H_i} \quad (106)$$

As mentioned earlier, an input  $\psi - \phi$  curve must be assumed. If the reasoning of Stepanoff (32) is followed, the input curve is a function only of the blade exit angle  $\beta_2$ . Since  $\beta_2$  is known from the impeller aerodynamic analysis, the input  $\psi - \phi$  curve is found from data presented in Section 7, Fig. 23. Corresponding values of  $\psi_{ix}$  and  $\phi_x$  are read from this curve at several points (both left and right of the design point). At each point  $\psi_{ix}$  and  $\phi_x$  are substituted into Eq. (106) and  $\psi_x$  is found. A new plot is then made of  $\psi_x$  versus  $\phi_x$ . Making use of the following equations, one can readily use the  $\psi_x - \phi_x$  curve to determine the actual predicted head-flow characteristic curve for the compressor being designed:

$$\psi = \frac{Hg}{U_2^2} \rightarrow H = \frac{\psi U_2^2}{g} \quad , \quad (107)$$

$$\phi = \frac{V_{R2}}{U_2} \rightarrow V_{R2} = \phi U_2 \quad , \quad (108)$$

$$Q = A_2 V_{R2} \quad , \quad (109)$$

$$A_2 = \left( \pi D_2 - \frac{z t_2}{\sin \beta_2} \right) h_2 \quad , \quad (110)$$

where

$A_2$  = available flow area at impeller exit,

$D_2$  = outer impeller diameter,

$z$  = number of vanes,

$t_2$  = blade thickness as exit,

$\beta_2$  = vane angle at exit,

$h_2$  = vane height at exit.

## 5. SURGING IN CENTRIFUGAL COMPRESSORS

The term surging is normally used to mean a periodic (not necessarily sinusoidal) pulsation in pressure. It exists when the head-capacity curve begins to move toward the zero-capacity point after having reached a maximum head. In Fig. 5, the maximum head occurs where the flow coefficient is about 0.06. When the flow coefficient is less than 0.06, the curve has a positive slope, which is not desirable. It is undesirable because, if flow were to momentarily increase for any reason, the pressure rise of the compressor would also increase and would tend to increase the flow still more. Conversely, if flow were to momentarily decrease for any reason, the pressure rise of the compressor would also decrease, which would tend to decrease the flow still further.

If the compressor were operating in the flow regime to the right of the maximum head in Fig. 5, this would mean a flow coefficient greater than 0.06, and the slope of the constant-speed characteristic curve would be negative. This would be desirable because, if flow were to momentarily increase, the pressure rise of the compressor would decrease and force the flow to decrease. Conversely, if flow were to momentarily decrease, the pressure rise of the compressor would increase and tend to increase the flow. Thus, when the compressor characteristic curve has a negative slope, restoring forces are present that tend to dampen perturbations. When the characteristic curve has a positive slope, the compressor tends to amplify perturbations. The designer should make certain that the compressor will operate in a region where the characteristic curve has a negative slope.

## 6. EXAMPLE OF AN IMPELLER DESIGN

In this section the design of an impeller will be described completely, since it is thought that a numerical example explains the procedures outlined in the previous sections better than lengthy written discussions. The conditions assumed are listed below:

Gas	Helium
Mass flow rate, $m$ , $\text{lb}_m/\text{hr}$	22,400
Pressure rise, $\Delta p$ , psi	2
Inlet pressure, $p_1$ , psia	500
Inlet temperature, $T_1$ , $^\circ\text{R}$	1010
Rotational speed, $N$ , rpm	4570
Ratio of gravitational constant to local acceleration of gravity, $g_c/g_L$	1

The head rise was determined from Eq. (12), given previously,

$$H = JT_1 C_p \frac{g_c}{g_L} \left[ \left( \frac{p_1}{p_2} \right)^{(1-k)/k} - 1 \right] ,$$

and the following relations:

$$C_p = 1.24 \text{ Btu}/\text{lb}_m \cdot ^\circ\text{R} ,$$

$$k = 1.67 ,$$

$$T_1 = 550 + 460 = 1010^\circ\text{R} ,$$

$$\frac{p_1}{p_2} = \frac{500}{502} = 0.996 ,$$

$$H = (778 \text{ ft}\cdot\text{lb}/\text{Btu})(1010^\circ\text{R})(1.24 \text{ Btu}/\text{lb}_m \cdot ^\circ\text{R}) \times \\ \times [(0.996)^{(1-1.67)/1.67} - 1] ,$$

$$H = 1560 \text{ ft} .$$

The inlet specific speed was determined from Eq. (13), given previously,

$$N_s = \frac{NQ^{1/2}}{H^{3/4}} ,$$

and the following relations:

$$\rho_1 = \frac{P_1}{ZRT_1} ,$$

$$p_c = 33.8 \text{ psi} ,$$

$$T_c = 9.5^\circ\text{R} ,$$

$$P_{R1} = \frac{P_1}{p_c} ,$$

$$T_{R1} = \frac{T_1}{T_c} ,$$

$$P_{R1} = \frac{500}{33.8} = 14.8 ,$$

$$T_{R1} = \frac{1010}{9.5} = 106 ,$$

$$Z_1 = 1 ,$$

when  $P_{R1} = 14.8$  and  $T_{R1} = 106$ , from charts similar to Fig. 1,

$$\rho_1 = \frac{(500 \text{ psi})(144 \text{ psf})}{(386 \text{ ft}\cdot\text{lb}_f/\text{lb}_m\cdot^\circ\text{R})(1010^\circ\text{R})}$$

$$\rho_1 = 0.185 \text{ lb}_m/\text{ft}^3 .$$

Then

$$Q = \frac{22,400 \text{ lb}_m/\text{hr}}{(0.185 \text{ lb}_m/\text{ft}^3)(60 \text{ min/hr})} = 2020 \text{ cfm} ,$$

$$N_s = \frac{(4570)(2020)^{1/2}}{(1560)^{3/4}}$$

$$N_s = 823 .$$

The isentropic fluid power required was then, from Eq. (14),

$$P = \frac{mH}{550}$$

$$P = \frac{(22,400 \text{ lb}_m/\text{hr})(1560 \text{ ft})}{(60 \text{ hr/min})(33,000 \text{ ft}\cdot\text{lb}_f/\text{lb}_m\cdot\text{min})}$$

$$P = 18 \text{ hp} .$$

The inlet pipe velocity was based on a 6-in., sched-40 (6.065 in. ID), inlet pipe and Eq. (15),

$$A_o = \frac{(3.142)(6.065)^2}{(4)(144)}$$

$$A_o = 0.206 \text{ ft}^2 ,$$

$$V_o = \frac{(2020 \text{ ft}^3/\text{min})}{(0.2006 \text{ ft}^2)(60 \text{ sec/min})}$$

$$V_o = 163 \text{ ft/sec} .$$

The impeller inlet velocity was based on  $\lambda = 1.03$ , that is, leakage from the diffuser back to the impeller inlet of 3% of the through flow, and Eq. (16),

$$V_1 = (1.03)(163)$$

$$V_1 = 168 \text{ ft/sec} .$$

The vane speed at the inlet was based on a vane inlet radius of 3.5 in. and Eq. (17),

$$U_1 = r_1 \omega ,$$

$$\omega = 479 \text{ rad/sec} ,$$

$$r_1 = 3.5 \text{ in.} ,$$

$$U_1 = \frac{(3.5)(479)}{12} ,$$

$$U_1 = 126 \text{ ft/sec} .$$

The relative velocity at the inlet was based on radial flow at the inlet, Fig. 2, and Eq. (18),

$$v_1 = [(V_1)^2 + (U_1)^2]^{1/2}$$

$$v_1 = [(168)^2 + (126)^2]^{1/2}$$

$$v_1 = 210 \text{ ft/sec} .$$

The inlet blade angle was based on Eq. (19),

$$\beta_1 = \arctan \frac{V_1}{U_1}$$

$$\beta_1 = \arctan \frac{168}{126}$$

$$\beta_1 = 53.1^\circ .$$

An exit angle  $\beta_2$  of  $65^\circ$  was chosen to give approximately maximum efficiency and a high head coefficient (see Figs. 3 and 4).

The outside diameter of the impeller was obtained from Eq. (34):

$$D_2 = \frac{2}{\omega} \left( \frac{Hg_L}{\psi} \right)^{1/2} ,$$

and the following values:

$$\psi = 0.50 \text{ (from Fig. 3) } ,$$

$$D_2 = \frac{2}{497} \left[ \frac{(1560)(32.2)}{0.50} \right]^{1/2}$$

$$D_2 = 1.28 \text{ ft} = 15.4 \text{ in.}$$

Therefore, let

$$D_2 = 15 \frac{1}{2} \text{ in.}$$

The number of vanes in the impeller was obtained from Eq. (35),

$$z = \xi \frac{D_2 + D_1}{D_2 - D_1} \sin \frac{\beta_1 + \beta_2}{2} ,$$

and the following values:

$$\xi = 10 \sin \frac{\beta_1 + \beta_2}{2}$$

$$\xi = 10 \sin \frac{53.1 + 65}{2}$$

$$\xi = 8.58 \quad ,$$

$$z = (8.50) \left( \frac{7 + 15.5}{15.7 - 7} \right) (0.858)$$

$$z = 19.5$$

or

$$z = 20 \text{ vanes} \quad .$$

For the slip factor, Eq. (36) was used:

$$S = 1 + \frac{1 + 0.6 \sin \beta_2}{0.5z(1 - 0.2835\delta)} \quad ,$$

$$\delta = \frac{D_1}{D_2}$$

$$\delta = \frac{7}{15.5}$$

$$\delta = 0.452 \quad ,$$

$$S = 1 + \frac{1 + 0.6 \sin 65^\circ}{(0.5)(20)[1 - (0.2835 \times 0.452)]}$$

$$S = 1.177 \quad .$$

For the radial component of the exit velocity, it was assumed that

$$V_{R2} = 140 \text{ ft/sec} \quad ,$$

and the impeller tip speed was taken from Eq. (37):

$$U_2 = r_2\omega$$

$$U_2 = (0.646)(479)$$

$$U_2 = 309 \text{ ft/sec} .$$

Then, with the use of Eqs. (38) and (39) and Fig. 7, the exit velocity was determined:

$$U_2 - V_{U2} = \frac{V_{R2}}{\tan \beta_2} ,$$

$$v_2 = [V_{R2}^2 + (U_2 - V_{U2})^2]^{1/2} ,$$

$$U_2 - V_{U2} = \frac{140}{\tan 65^\circ}$$

$$U_2 - V_{U2} = 65.3 \text{ ft/sec} ,$$

$$v_2 = [(140)^2 + (65.3)^2]^{1/2}$$

$$v_2 = 154 \text{ ft/sec} .$$

The fluid absolute velocity at the exit was then determined based on Fig. 8, Eqs. (40) through (43), and the following values:

$$V_{U2} = U_2 - (U_2 - V_{U2})$$

$$V_{U2} = 309 - 65.3$$

$$V_{U2} = 244 \text{ ft/sec} ,$$

$$V'_{U2} = \frac{V_{U2}}{S}$$

$$V'_{U2} = \frac{244}{1.177}$$

$$V'_{U2} = 207 \text{ ft/sec} ,$$

$$V'_2 = [(V_{R2})^2 + (V'_{U2})^2]^{1/2}$$

$$V'_2 = [(140)^2 + (207)^2]^{1/2}$$

$$V'_2 = 250 \text{ ft/sec} ,$$

$$v'_2 = [(V_{R2})^2 + (U_2 - V'_{U2})^2]^{1/2}$$

$$v'_2 = [(140)^2 + (309 - 207)^2]^{1/2}$$

$$v'_2 = 173 \text{ ft/sec} ,$$

$$\gamma'_2 = \arcsin \frac{V_{R2}}{V'_2}$$

$$\gamma'_2 = \arcsin \frac{140}{250}$$

$$\gamma'_2 = 34^\circ .$$

The head produced by the impeller was estimated with the use of Eq. (57),

$$H_I = \frac{1}{2g_c} (V_2'^2 - V_1^2 + U_2^2 - U_1^2 + v_1^2 - v_2'^2) ,$$

and the following values:

$$H_I = \frac{1}{(2)(32.2)} [(250)^2 - (168)^2 + (309)^2 - (126)^2 + (210)^2 - (173)^2] ,$$

$$H_I = 1990 \text{ ft (ideal rise) } ,$$

$$\eta_o \cong 0.80 ,$$

since

$$N_s = 823 ,$$

$$H = \eta_o H_I$$

$$H = (0.80)(1990)$$

$$H = 1590 \text{ ft (actual predicted head rise) } .$$

The impeller outlet static pressure head and pressure were obtained using Eqs. (59) and (61) and the related values:

$$H_s = \frac{1}{2g_c} (U_2^2 - U_1^2 + v_1^2 - v_2'^2)$$

$$H_s = \frac{1}{2(32.2)} [(309)^2 - (126)^2 + (210)^2 - (173)^2]$$

$$H_s = 1460 \text{ ft (isentropic head) } ,$$

$$P_{2s} = P_1 \left( \frac{H_s}{J\Gamma_1 C_P \frac{g_c}{g_L}} + 1 \right)^{k/(k-1)}$$

$$p_{2s} = 500 \text{ psi} \left[ \frac{1460 \text{ ft}}{(778 \text{ ft}\cdot\text{lb/Btu})(1010^\circ\text{R})(1.24 \text{ Btu/lb}_m\cdot^\circ\text{R})} + 1 \right]$$

$$p_{2s} = 501.85 \text{ psi} .$$

The impeller exit temperature was determined from the isentropic pressure ratio [Eq. (62)]:

$$T_2 = T_1 \left( \frac{p_{2s}}{p_1} \right)^{(k-1)/k}$$

$$T_2 = 1010(1.0037)^{0.40}$$

$$T_2 = 1011.5^\circ\text{R} \rightarrow \Delta T = 1.5^\circ\text{F} .$$

The temperature rise was determined from the Gas Tables (18) and Eqs. (63) and (64):

$$p_{R1} = \frac{p_1}{p^*} ,$$

$$p_{R2} = \frac{p_{2s}}{p^*} = p_{R1} \left( \frac{p_{2s}}{p_1} \right) ,$$

$$p_{R1} = 58.85 \text{ at } 1010^\circ\text{R} \text{ from } \underline{\text{Gas Tables}} \text{ (18)} ,$$

$$p_{R2s} = (58.85)(1.0037)$$

$$p_{R2s} = 59.07 ,$$

$$T_2 = 1000 + \frac{1.76}{15.43} (100) \text{ from } \underline{\text{Gas Tables}} \text{ (18) at } p_{R2} = 59.07$$

$$T_2 = 1011.4^\circ\text{R} \rightarrow \Delta T = 1.4^\circ\text{F} .$$

The impeller exit density was obtained from Eq. 65:

$$\rho_2 = \frac{P_2}{Z_2 R T_2} ;$$

$$P_2 \cong P_1$$

and

$$T_2 \cong T_1 ,$$

hence

$$Z_2 \cong Z_1 = 1 .$$

Then

$$\rho_2 = \frac{(501.85)(144)}{(386)(1011.4)}$$

$$\rho_2 = 0.185 \text{ lb}_m/\text{ft}^3 .$$

The vane heights at the inlet and the outlet were determined from Eqs. (69) and (72). Since the density changes very little through the impeller, the volume flow will also be constant. The flow area required at inlet is the same as the inlet pipe area:

$$A_1 = A_o = 28.89 \text{ in.}^2 ,$$

and therefore

$$h_1 = \frac{A_1}{\pi D_1 \sin \beta_1} .$$

If  $t_1 = 1/8$  in., then

$$h_1 = \frac{28.89}{(3.14)(7) - \frac{(20)(0.125)}{\sin(53.1^\circ)}}$$

$$h_1 = 1.53 \text{ in.}$$

At the exit,

$$A_2 = \frac{\lambda Q}{V_{R2}}$$

$$A_2 = \frac{(1.03)(2020 \text{ ft}^3/\text{min})}{(140 \text{ ft}/\text{sec})(60 \text{ sec}/\text{min})} = 0.248 \text{ ft}^2 = 35.7 \text{ in.}^2$$

If  $t_2 = 1/4$  in., then

$$h_2 = \frac{A_2}{\pi D_2 - \frac{z t_2}{\sin \beta_2}}$$

$$h_2 = \frac{35.7}{(3.14)(15.5) - \frac{(20)(0.25)}{\sin 65^\circ}}$$

$$h_2 = 0.83 \text{ in.}$$

The velocity distribution along the driving face of the impeller vanes was determined from Eqs. (84) through (89):

$$q_d = \left\{ u^2 + \frac{2C_o^2}{k-1} \left[ 1 - \left( \frac{p_a}{p_o} + \frac{\Delta p}{2p_o} \right)^{(k-1)/k} \right] \right\}^{1/2},$$

$$p_a = p_{a1} + \frac{p_{a2} - p_{a1}}{r_2 - r_1} (r - r_1)$$

$$p_a = 500 + \frac{501.85 - 500}{7.75 - 3.5} (r - 3.5)$$

$$p_a = 498.48 + 0.435 r \quad ,$$

$$P = \frac{18}{0.8}$$

$$P = 22.5 \text{ hp} \quad ,$$

$$\tau = \frac{P}{\omega}$$

$$\tau = \frac{(22.5 \text{ hp})(550 \text{ ft}\cdot\text{lb}/\text{sec}\cdot\text{hp})}{479/\text{sec}}$$

$$\tau = 25.8 \text{ ft}\cdot\text{lb}$$

$$\tau = F_{\theta} \bar{r} \rightarrow F_{\theta} = \frac{\tau}{\bar{r}} \quad ,$$

$$\bar{r} = \frac{7.75 + 3.5}{2}$$

$$\bar{r} = 5.625 \text{ in.} = 0.469 \text{ ft} \quad ,$$

$$F_{\theta} = \frac{25.8}{0.469}$$

$$F_{\theta} = 55.0 \text{ lb} \quad ,$$

$$F_{\theta N} = \frac{F_{\theta}}{z}$$

$$F_{\theta N} = \frac{55.0}{20}$$

$$F_{\theta N} = 2.75 \text{ lb per blade} ,$$

$$A_r = \frac{h_2 + h_1}{2} (r_2 - r_1)$$

$$A_r = \frac{(0.83 + 1.53)}{2} (7.75 - 3.5)$$

$$A_r = 5.015 \text{ in.}^2 ,$$

$$\Delta p = \frac{2.75}{5.015}$$

$$\Delta p = 0.548 \text{ psi} ,$$

$$C_o = (g_c k R T_o)^{1/2} ,$$

$$k = 1.67 ,$$

$$R = 386 \text{ ft} \cdot \text{lb}_f / \text{lb}_m \cdot ^\circ\text{R} ,$$

$$C_o = [(32.2)(1.67)(386)(1010)]^{1/2}$$

$$C_o = 4580 \text{ ft/sec} \rightarrow C_o^2 = 2.098 \times 10^7 ,$$

$$p_o = p + \frac{\rho V^2}{2g_c}$$

$$p_o = 500 + (0.5)(0.185)(163)^2 \left( \frac{1}{32.2} \right) \left( \frac{1}{144} \right)$$

$$p_o = 500.53 \text{ psia} ,$$

$$u^2 = \frac{r^2 \omega^2}{144}$$

$$u^2 = \frac{r^2 (229,440)}{144} ,$$

$$q_d = \left\{ 0.016 \times 10^5 r^2 + \frac{(2)(2.098 \times 10^7)}{(1.67 - 1)} \times \right. \\ \left. \times \left[ 1 - \left( \frac{498.48 + 0.435r + 0.274}{500.53} \right)^{(1.67-1)/1.67} \right]^{1/2} \right\}$$

$$q_d = \left\{ 0.0016r^2 + 62.6 [1 - (0.9965 + 0.0008691r)^{0.401}] \right\}^{1/2} \times 10^3 ,$$

$$r_{\max} = r_2$$

$$r_{\max} = 7.75 ,$$

$$(0.9965 + 0.0008691r)^{0.401} = [0.995 + (0.0008691)(7.75)]^{0.401} ,$$

$$0.401 \log_{10} 1.0032 = (0.401)(0.0013875) = 0.000556 ,$$

$$\text{Antilog } (0.000556) = 1.0013 .$$

Then

$$q_d = 10^3 [(0.0016)(60.1) + 62.6 (1 - 1.0013)]^{1/2}$$

$$q_d = 122 \text{ fps} .$$

These calculations give a relative velocity along the driving face of the exit vanes of 122 fps. Since the relative velocity is positive at the exit, it must be positive at any radius. Therefore, secondary vanes are not necessary in this impeller. The impeller layout is shown in Fig. 20.

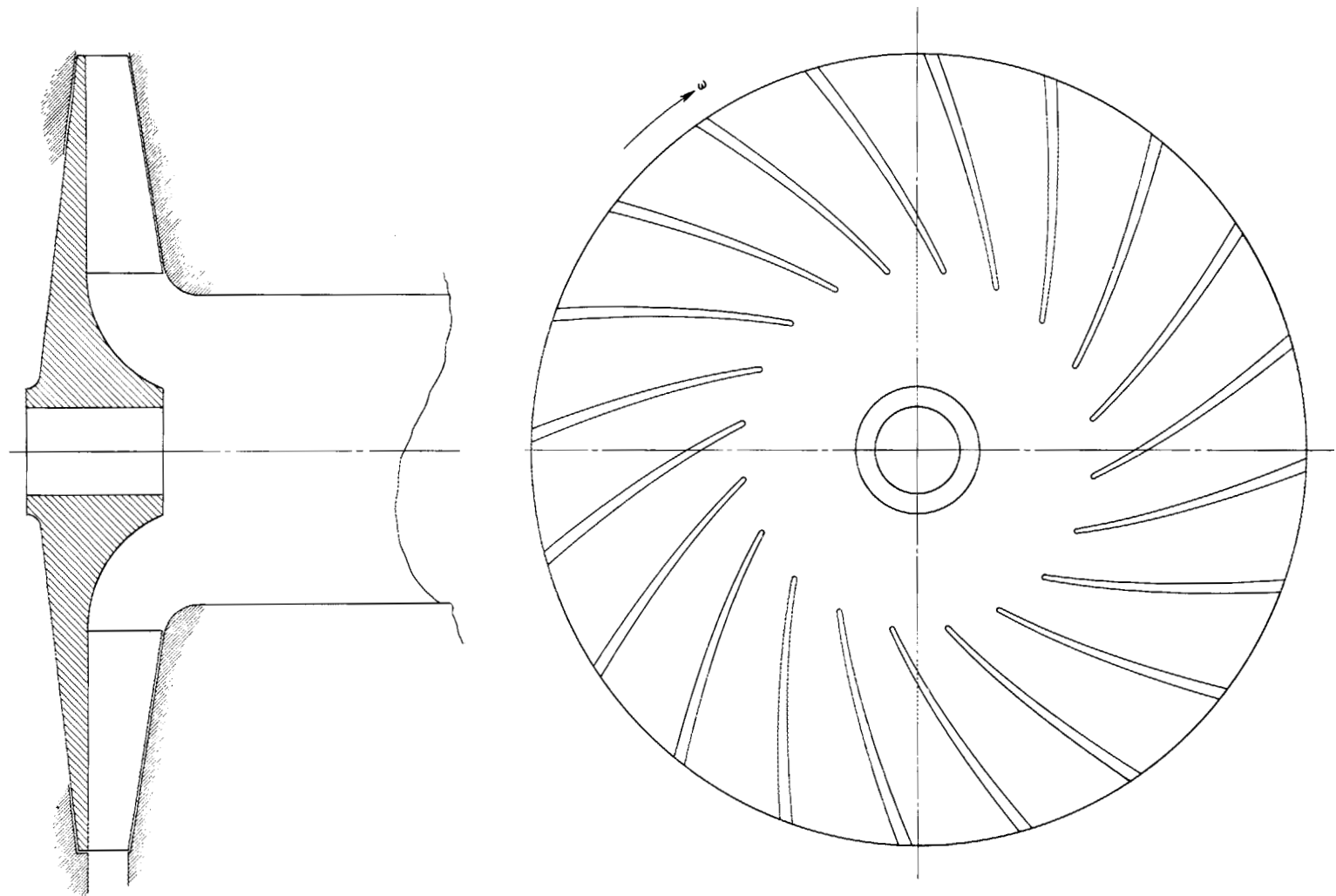


Fig. 20. Example of an Impeller Layout.

## 7. EXAMPLE OF A CASING DESIGN

In the previous section an impeller was designed for certain assumed requirements. A casing will now be designed to carry the fluid to and from the impeller. Since a combination of constant-velocity volute and conical diffuser are quite often used, it would seem logical to use such a combination for an example of a design. There are, of course, several other types of collector-diffuser combinations (vaneless diffuser and volute, etc.) which could perfectly well be used for such a compressor, but only the volute-conical diffuser type will be discussed here. For the other types of collector-diffuser combinations, the goals are exactly the same. The collector-diffuser should take flow from the impeller and efficiently change its direction and speed to that of the exit pipe.

Volute Design

The volute tongue diameter was determined from Eq. (91):

$$D_3 = 1.15 D_2$$

$$D_2 = 15.5 \text{ in.}$$

$$D_3 = (15.5)(1.15)$$

$$D_3 = 17.8 \text{ in.}$$

The average casing velocity was calculated with the use of Eq. (92):

$$V_v = \sigma V_2' ,$$

$$\gamma_2' = 34^\circ ,$$

$$V_2' = 250 \text{ ft/sec} ,$$

$$\sigma = 0.52 \text{ from Fig. 12 at } \gamma_2' = 34^\circ ,$$

$$V_v = (0.52)(250) ,$$

$$V_v = 130 \text{ fps} .$$

The volute outlet area parameters were determined from Eqs. (94) through (98). The static pressure and temperature calculations follow:

$$H_v = \eta_o \left[ H_s + \frac{1}{2g_c} (V_2'^2 - V_v^2) \right]$$

$$H_v = 0.80 \left\{ 1460 + \frac{1}{(2)(32.2)} [(250)^2 - (130)^2] \right\}$$

$$H_v = 1735 \text{ ft} ,$$

$$p_v = p_1 \left( \frac{H_v}{\frac{J T_1 C_p}{g_c} + 1} \right)^{k/(k-1)}$$

$$p_v = 500 \left[ \frac{1735}{(778)(1010)(1.24)} + 1 \right]^{2.5}$$

$$p_v = 502.23 \text{ psia} ,$$

$$T_v = T_1 \left( \frac{p_v}{p_1} \right)^{(k-1)/k}$$

$$T_v = 1010 \left( \frac{502.23}{500} \right)^{0.40} = 1010(1.0045)^{0.40}$$

$$T_v = 1011.8^\circ\text{R} .$$

The average density in the volute is

$$\rho_v = \frac{p_v}{ZRT_v} ,$$

and

$$Z = 1 \quad ,$$

since  $p_v \cong p_1$  and  $T_v \cong T_1$ ; therefore

$$\rho_v = \frac{(502.23)(144)}{(386)(1011.8)}$$

$$\rho_v = 0.185 \text{ lb}_m/\text{ft}^3 \quad .$$

The volute flow at the volute outlet is

$$Q_4 = \frac{22,400}{(0.185)(60)}$$

$$Q_4 = 2020 \text{ ft}^3/\text{min} \quad .$$

The volute outlet area is

$$A_4 = \frac{Q_4}{V_v}$$

$$A_4 = \frac{2020 \text{ ft}^3/\text{min}}{130 \text{ ft}/\text{sec}} \left( \frac{1}{60} \text{ min}/\text{sec} \right)$$

$$A_4 = 0.259 \text{ ft}^2$$

or

$$A_4 = 37.3 \text{ in.}^2 \quad .$$

The cross-sectional area required at various angles in the volute is, from Eq. (99),

$$A_{\Delta} = A_4 \frac{\Delta}{360} .$$

If the cross section of the volute is circular at any angle, then

$$D_{\Delta} = \left( \frac{4A_{\Delta}}{\pi} \right)^{1/2}$$

$$D_{\Delta} = \left( \frac{4A_4 \Delta}{(\pi)(360)} \right)^{1/2}$$

$$D_{\Delta} = \left( \frac{A_4}{9\pi} \right)^{1/2} (\Delta)^{1/2}$$

$$D_{\Delta} = 0.364 (\Delta) ,$$

where  $D_{\Delta}$  is the diameter of the cross section at angle  $\Delta$ . The volute tongue angle is

$$\theta_v = \gamma'_2$$

$$\theta_v = 34^{\circ} .$$

#### Diffuser Design

The diffuser angle,  $\theta_D$ , was taken as  $8^{\circ}$  and the inlet area

$$A_4 = 37.3 \text{ in.}^2 .$$

The exit from the diffuser was assumed to be an 8-in., sched.-40 (7.981-in.-ID) pipe, with an outlet area

$$A_5 = \frac{3.142}{4} (7.981)^2$$

$$A_5 = 50.0 \text{ in.}^2 .$$

The diffuser length was calculated from Eq. (100):

$$L_D = \frac{D_5 - D_4}{2 \tan \frac{\theta_D}{2}}$$

$$L_D = \frac{7.981 - 6.92}{2 \tan \frac{8^\circ}{2}}$$

$$L_D = 7.59 \text{ in.}$$

The results of the volute design are summarized in Table 1, and Fig. 21 gives a layout of the casing as an example of the design. The predicted head-flow characteristics for the design are given in Figs. 22 and 23 and in Table 2.

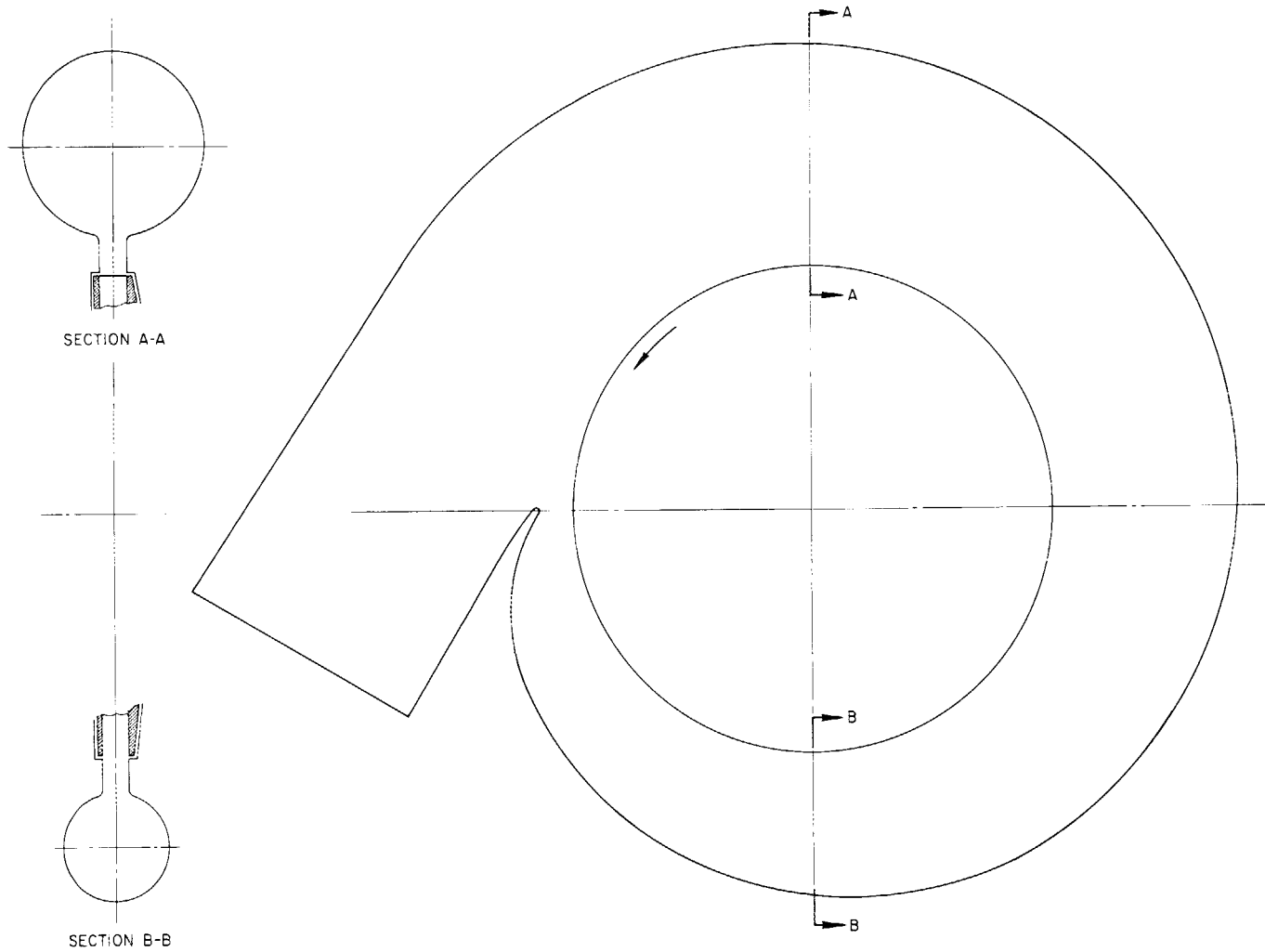
Table 1. Volute Design Data

Angle Measured from Tongue (degrees)	Diameter of Cross Section (in.)	Cross-Sectional Area (in. <sup>2</sup> )
0	0	0
30	1.99	3.1
60	2.82	6.3
90	3.46	9.4
120	3.99	12.5
150	4.46	15.6
180	4.88	18.7
210	5.28	21.90
240	5.64	25.0
270	5.97	28.0
300	6.30	31.2
330	6.62	34.4
360	6.92	37.3

Table 2. Head Losses for Volute Design

Flow Coefficient	Input Head Coefficient	Loss of Conversion	Friction Loss	Additional Loss in Volute	Entrance Loss	Output Head Coefficient
0.1	0.65	0.02	0.00098	0.099	0.006	0.524
0.2	0.62	0.02	0.0039	0.054	0.016	0.526
0.3	0.59	0.02	0.0088	0.019	0.021	0.521
0.4	0.56	0.02	0.0156	0.002	0.013	0.508
0.453 <sup>a</sup>	0.54	0.02	0.020	0	0	0.50
0.5	0.52	0.02	0.024	0.002	-0.007	0.481
0.6	0.49	0.02	0.035	0.019	-0.0188	0.435
0.7	0.46	0.02	0.048	0.054	-0.043	0.381
0.8	0.43	0.02	0.062	0.099	-0.079	0.328

<sup>a</sup>Design flow coefficient.



70

Fig. 21. Example of Casing Layout.

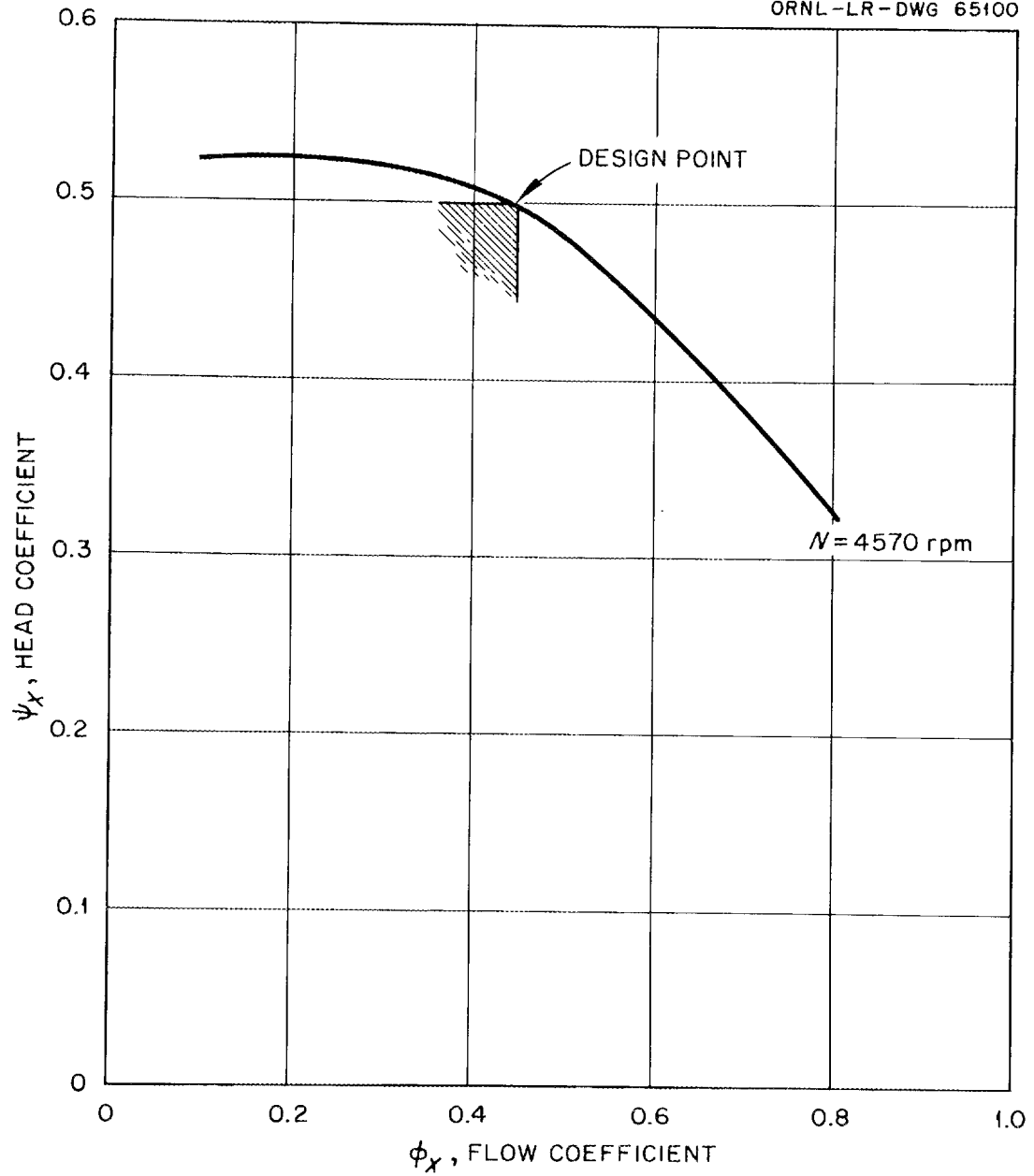
UNCLASSIFIED  
ORNL-LR-DWG 65100

Fig. 22. Predicted Coefficients for Design.

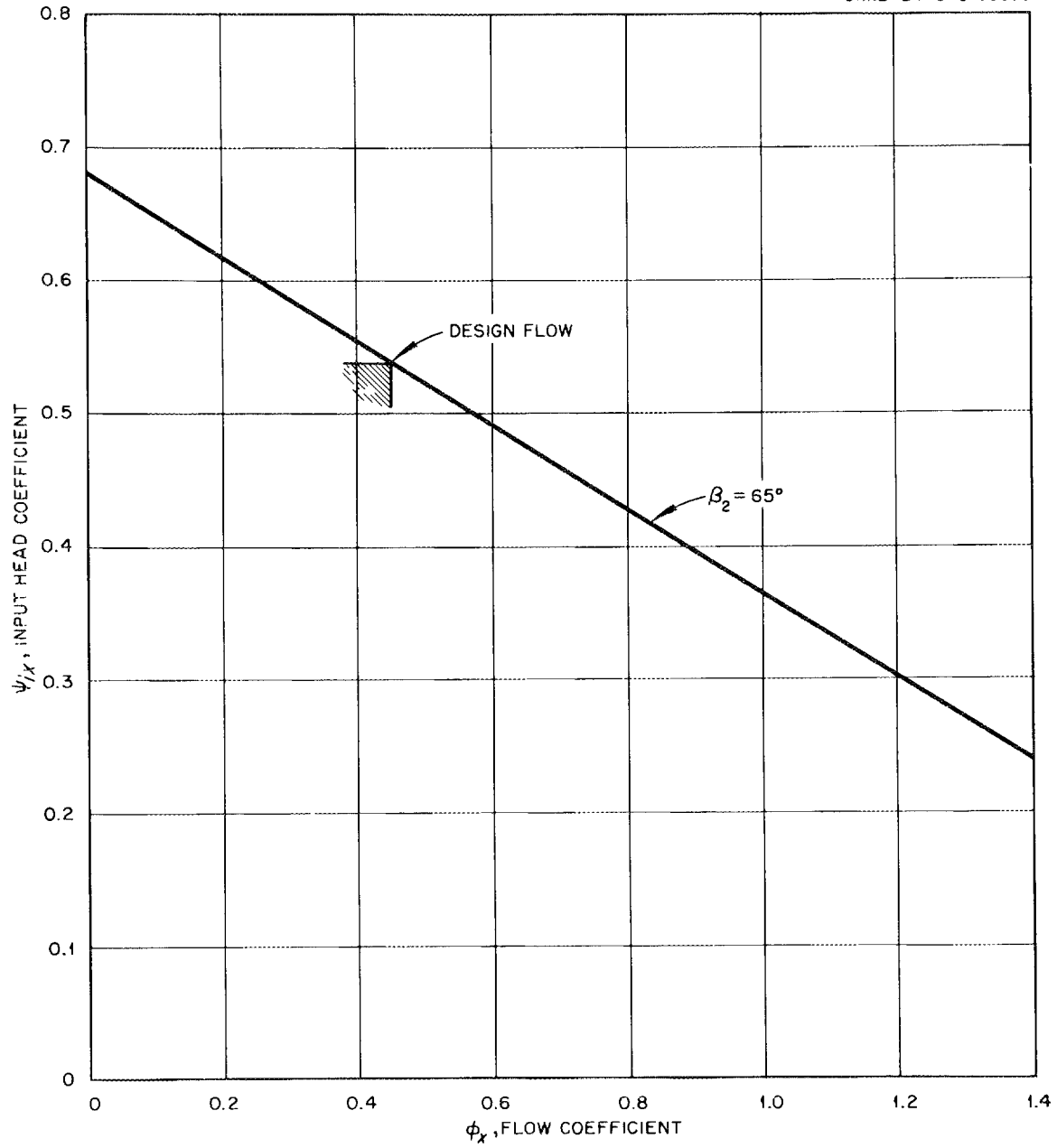
UNCLASSIFIED  
ORNL-LR-DWG 65098

Fig. 23. Input Characteristics for Design.

### 3. SUMMARY

Procedures have been given for the aerodynamic-thermodynamic design of centrifugal compressors. A complete example of a design has also been given that illustrates use of the equations. Each design will, no doubt, bring up problems that are unique. It is in this area that the designer must learn to alter certain steps in the design procedures. The designer must, of course, also decide, before a design is started, what is to be the most important factor in his design philosophy; that is, he must select from factors such as economy of operation, low initial capital outlay, efficiency of operation, maximum output, and ease of manufacture and assembly.

Most of the important equations have been developed from the basic laws of fluid flow and thermodynamics. All assumptions and approximations have been listed in the derivations so that the equations will be applicable in other situations. The compressibility factor used in conjunction with the ideal gas equation is probably the most accurate method presently known for relating properties of a gas. Although some of the steps in the design procedure may seem to be unnecessary, they are included in order for the procedures to be general.

The most obvious application of this work can be made by the compressor designer. An application that is perhaps not so obvious can be made by the development engineer. He must write specifications and evaluate proposals for centrifugal compressors. It is in this area that the design procedures given should be of particular usefulness.

## ACKNOWLEDGMENTS

This report was presented to the Graduate Council of the University of Tennessee in partial fulfillment of the requirements for the Degree of Master of Science. It was edited before publication in its present form to comply with the established style of Oak Ridge National Laboratory reports.

The author wishes to give particular credit to Professor W. K. Stair of the University of Tennessee who carefully read the several drafts of this paper and offered constructive criticism that materially affected the arrangement and scope of the report.

## BIBLIOGRAPHY

1. H. H. Anderson, The Hydraulic Design of Centrifugal Pumps and Water Turbines, ASME Paper No. 61-WA-320.
2. O. E. Baljé, A Contribution to the Problem of Designing Radial Turbo-machines, Transactions of the ASME, May 1952.
3. O. E. Baljé, A Study on Design Criteria and Matching of Turbomachines, ASME Paper No. 60-WA-230.
4. O. E. Baljé, A Study on Design Criteria and Matching of Turbomachines, ASME Paper No. 60-WA-231.
5. R. C. Binder, Advanced Fluid Dynamics and Fluid Machinery, Prentice-Hall, Inc., New York, 1951.
6. W. B. Brown, Friction Coefficients in a Vaneless Diffuser, NACA Technical Note No. 1311, Washington, 1947.
7. W. B. Brown and G. R. Bradshaw, Design and Performance of Family of Diffusing Scrolls with Mixed-Flow Impeller and Vaneless Diffuser, NACA Technical Note No. 1568.
8. R. O. Bullock, W. W. Wilcox, and J. J. Moses, Experimental and Theoretical Studies of Surging in Continuous Flow Compressors, NACA Technical Note No. 1213, Washington, 1947.
9. A. B. Cambel and B. H. Jennings, Gas Dynamics, McGraw-Hill Book Company, Inc., New York, 1958.
10. A. H. Church, Centrifugal Pumps and Blowers, John Wiley and Sons, New York, 1954.
11. G. T. Csanady, Radial Forces in a Pump Impeller Caused by a Volute Casing, ASME Paper No. 61-WA-77.
12. H. Davis, H. Kottas, and A. M. G. Moody, The Influence of Reynolds Number on the Performance of Turbomachinery, Transactions of the ASME, 1951.
13. W. T. Furgerson, Parallel Operation of Turbo-Compressors in a Common System, ASME Symposium on Compressor Stall, Surge and System Response, Houston, Texas, March 6-9, 1960.
14. J. T. Hamrick, Some Aerodynamic Investigations in Centrifugal Impellers, Transactions of the ASME, April 1956, p. 591.

15. J. T. Hamrich, A. Ginsburg, and W. M. Osborn, Method of Analysis for Compressible Flow Through Mixed-Flow Centrifugal Impellers of Arbitrary Design, NACA, Report 1082, Lewis Flight Propulsion Laboratory, Cleveland, Ohio, 1952.
16. A. T. Ippen, The Influence of Viscosity on Centrifugal Pump Performance, Transactions of the ASME, November 1946.
17. B. H. Jennings and W. L. Rogers, Gas Turbine Analysis and Practice, McGraw-Hill Book Company, Inc., New York, 1953.
18. J. H. Keenan and J. Kaye, Gas Tables, John Wiley and Sons, Inc., New York, 1957.
19. A. Kovats, Calculation of Radial-Flow-Impeller Performance Curves by the Modified Aerofoil Theory, ASME Paper No. 58-A-86.
20. F. H. Linley, How to Use Specific Speed, Machine Design, October 27, 1960.
21. K. E. Nichols, D. G. McPherson, and O. E. Balje', Study of Turbine and Turbopump Design Parameters, Final Report - Volume IV, Sunstrand Turbo, Sunstrand Corporation, Nov. 20, 1959.
22. H. Peters, Conversion of Energy in Cross-Sectional Divergences Under Different Conditions of Inflow, NACA Technical Note No. 737, Washington, 1934.
23. C. Pfeleiderer, Die Kreiselpumpen fur Flussigkeiten und Gase, Springer-Verlag, Berlin, Germany, 1955.
24. W. K. Ritter, A. Ginsburg, and A. G. Redlitz, Effects of Axial-Plane Curvature and Passage-Area Variation on Flow Capacity of Radial-Discharge Impeller with Conventional Inlet Buckets, NACA Technical Note No. 1068, Washington, 1946.
25. M. J. Schilhansl, Stress Analysis of a Radial-Flow Rotor, ASME Paper No. 60-WA-200.
26. J. D. Stanitz, Approximate Design Method for High-Solidity Blade Elements in Compressors and Turbines, NACA Technical Note 2408, Washington, 1951.
27. J. D. Stanitz, Centrifugal Compressors, Gas Turbine and Free Piston Engine Lectures, Department of Mechanical and Industrial Engineering, University of Michigan, Ann Arbor, Michigan, July 7, 1958.

28. J. D. Stanitz, One-Dimensional Compressible Flow in Vaneless Diffusers of Radial- and Mixed-Flow Centrifugal Compressors, Including Effects of Friction, Heat Transfer and Area Change, NACA Technical Note 2610, Washington, January 1952.
29. J. D. Stanitz and G. O. Ellis, Two-Dimensional Compressible Flow in Centrifugal Compressors with Straight Blades, NACA, Report 954, Lewis Flight Propulsion Laboratory, Cleveland, Ohio, 1950.
30. A. J. Stepanoff, Inlet Guide Vane Performance of Centrifugal Blowers, ASME Paper No. 60-WA-130.
31. A. J. Stepanoff, Leakage Loss and Axial Thrust in Centrifugal Pumps, Transactions of the ASME HYD-54-5.
32. A. J. Stepanoff, Turboblowers, John Wiley and Sons, 1955, New York.
33. A. J. Stepanoff and H. A. Stahl, Dissimilarity Laws in Centrifugal Pumps and Blowers, ASME Paper No. 60-WA-145.
34. W. L. Stewart, W. J. Whitney, and R. Y. Wong, A Study of Boundary-Layer Characteristics of Turbomachine Blade Rows and Their Relation to Over-All Blade Loss, ASME Paper No. 59-A-23.
35. W. C. Swan, A Practical Method of Predicting Transonic-Compressor Performance, ASME Paper No. 60-WA-191.
36. W. E. Trumpler, R. W. Frederick, and P. R. Trumpler, Heat-Transfer Rates in Centrifugal Compressors and the Effect of Internal Liquid Cooling on Performance, Transactions of the ASME, Volume 72, August 1950.
37. J. M. Watson, To Move Air-Equations Find the Right Impeller, Product Engineering, January 9, 1961.
38. C. H. Wu, A General Theory of Three-Dimensional Flow in Subsonic and Supersonic Turbomachines of Axial-, Radial-, and Mixed-Flow Types, NACA Technical Note 2604, Washington, January 1952.



ORNL-3294

UC-80 -- Reactor Technology  
TID-4500 (18th ed.)Internal Distribution

- |                         |                                                                     |
|-------------------------|---------------------------------------------------------------------|
| 1. S. E. Beall          | 39. M. I. Lundin                                                    |
| 2. M. Bender            | 40. H. G. MacPherson                                                |
| 3. D. S. Billington     | 41-69. W. D. Manly                                                  |
| 4. E. P. Blizard        | 70. A. P. Marquardt                                                 |
| 5. A. L. Boch           | 71. K. Z. Morgan                                                    |
| 6. C. J. Borkowski      | 72. M. L. Nelson                                                    |
| 7. E. J. Breeding       | 73. P. Patriarca                                                    |
| 8. R. B. Briggs         | 74. A. M. Perry                                                     |
| 9. W. F. Boudreau       | 75. D. Phillips                                                     |
| 10. C. D. Cagle         | 76. M. E. Ramsey                                                    |
| 11. W. L. Carter        | 77. M. W. Rosenthal                                                 |
| 12. C. J. Claffey       | 78. G. Samuels                                                      |
| 13. H. C. Claiborne     | 79. H. W. Savage                                                    |
| 14. W. G. Cobb          | 80. A. W. Savolainen                                                |
| 15-17. G. T. Colwell    | 81. O. Sisman                                                       |
| 18. J. M. Corum         | 82. E. D. Shipley                                                   |
| 19. J. A. Cox           | 83. M. J. Skinner                                                   |
| 20. F. L. Culler        | 84. A. H. Snell                                                     |
| 21. I. T. Dudley        | 85. E. Storto                                                       |
| 22. J. L. Fowler        | 86. J. A. Swartout                                                  |
| 23. A. P. Fraas         | 87. E. H. Taylor                                                    |
| 24. J. H. Frye          | 88. D. B. Trauger                                                   |
| 25. W. R. Grimes        | 89. D. R. Vondy                                                     |
| 26. A. G. Grindell      | 90. C. S. Walker                                                    |
| 27. W. O. Harms         | 91. J. L. Wantland                                                  |
| 28. N. Hilvety          | 92. G. M. Watson                                                    |
| 29. A. Hollaender       | 93. A. M. Weinberg                                                  |
| 30. A. S. Householder   | 94. J. H. Westsik                                                   |
| 31. W. H. Jordan        | 95. L. V. Wilson                                                    |
| 32. C. P. Keim          | 96. F. C. Zapp                                                      |
| 33. M. T. Kelley        | 97-99. Central Research Library                                     |
| 34. T. S. Kress         | 100-102. ORNL-Y-12 Technical Library,<br>Document Reference Section |
| 35. J. A. Lane          | 103-127. Laboratory Records Department                              |
| 36. C. E. Larson (K-25) | 128. Laboratory Records, LRD-RC                                     |
| 37. M. E. LaVerne       |                                                                     |
| 38. R. S. Livingston    |                                                                     |

External Distribution

- 129-131. W. F. Banks, Allis-Chalmers Mfg. Co.  
132-134. P. B. Bush, Kaiser Engineers

- 135. R. A. Charpie, UCC Research Administration, New York, N.Y.
- 136. W. R. Cooper, Tennessee Valley Authority
- 137-138. David F. Cope, Reactor Division, AEC, ORO
- 139-140. R. W. Coyle, Vallecitos Atomic Laboratory
- 141. E. Creutz, General Atomic
- 142-144. R. B. Duffield, General Atomic
- 145. H. L. Falkenberry, Tennessee Valley Authority
- 146. D. H. Fax, Westinghouse Atomic Power Division
- 147. M. Janes, National Carbon Research Laboratories, Cleveland, Ohio
- 148. T. Jarvis, Ford Instrument Co.
- 149. James R. Johnson, Minnesota Mining and Manufacturing Company, Saint Paul, Minn.
- 150. Richard Kirkpatrick, AEC, Washington
- 151. C. W. Kuhlman, United Nuclear Corp.
- 152-153. H. Lichtenburger, General Nuclear Engineering Corp.
- 154. J. P. McGee, Bureau of Mines, Appalachian Experiment Station
- 155. R. W. McNamee, Manager, UCC Research Administration, New York, N.Y.
- 156. S. G. Nordlinger, AEC, Washington
- 157. R. E. Pahler, High-Temperature Reactor Branch, Reactor Division, AEC, Washington
- 158. H. B. Rahner, Savannah River Operations Office
- 159. Corwin Rickard, General Atomic
- 160. M. T. Simnad, General Atomic
- 161. Nathaniel Stetson, Savannah River Operations Office
- 162. Donald Stewart, AEC, Washington
- 163. Philip L. Walker, Pennsylvania State University
- 164. R. E. Watt, Los Alamos Scientific Laboratory
- 165-166. W. L. Webb, East Central Nuclear Group, Inc.
- 167. C. E. Winters, UCC, Cleveland, Ohio
- 168. Lloyd R. Zumwalt, General Atomic
- 169. Division of Research and Development, AEC, ORO
- 170-773. Given distribution as shown in TID-4500 (18th ed.) under Reactor Technology category (75 copies - OES)